

Simultaneously Transmitting and Reflecting RIS (STAR-RIS) Assisted Multi-Antenna Covert Communications: Analysis and Optimization

Han Xiao, *Student Member, IEEE*, Xiaoyan Hu*, *Member, IEEE*,
Pengcheng Mu, *Member, IEEE*, Wenjie Wang, *Member, IEEE*, Tong-Xing Zheng, *Member, IEEE*,
Kai-Kit Wong, *Fellow, IEEE*, Kun Yang, *Fellow, IEEE*

Abstract—This paper investigates the multi-antenna covert communications assisted by a simultaneously transmitting and reflecting reconfigurable intelligent surface (STAR-RIS). In particular, to shelter the existence of covert communications between a multi-antenna transmitter and a single-antenna receiver from a warden, a friendly full-duplex receiver with two antennas is leveraged to make contributions where one antenna is responsible for receiving the transmitted signals and the other one transmits the jamming signals with a varying power to confuse the warden. Considering the worst case, the closed-form expression of the minimum detection error probability (DEP) at the warden is derived and utilized in a covert constraint to guarantee the system performance. Then, we formulate an optimization problem maximizing the covert rate of the system under the covertness constraint and quality of service (QoS) constraint with communication outage analysis. To jointly design the active and passive beamforming of the transmitter and STAR-RIS, an iterative algorithm based on semi-definite relaxation (SDR) method and Dinkelbach's algorithm is proposed to effectively solve the non-convex optimization problem. Simulation results show that the proposed STAR-RIS-assisted scheme highly outperforms the case with conventional RIS, which validates the effectiveness of the proposed algorithm as well as the superiority of STAR-RIS in guaranteeing the covertness of wireless communications.

Index Terms—Covert communication, STAR-RIS, multi-antenna, full-duplex, jamming.

I. INTRODUCTION

With the advent of 5G era, people are becoming increasingly dependent on wireless communications driven by the advanced communications and data processing techniques. Massive important and sensitive information, e.g., ID information, confidential documents, etc., are transmitted over open wireless networks, which aggravates the eavesdropping risk. Hence, people pay more and more attention to the problem of information security. Physical layer security (PLS) as a critical technology in protecting private information from eavesdropping attacks has drawn great attention in recent years [1]–[3]. However, PLS techniques cannot perform well in scenarios

with covertness requirements, e.g., secret military operations, since PLS is only able to protect the content information of wireless communications but is unable to hide the existence of communications [4], [5]. Recently, the technology of covert communications has emerged as a new security paradigm and attracted significant research interests in both civilian and military applications [6], which can shelter the existence of communications between transceivers and provide a higher level of security for wireless communication systems.

A. Related Works

As a breakthrough work, [7] first proved the fundamental limit of covert communications over additive white Gaussian noise (AWGN) channels from the perspective of information theory. It demonstrates that $O(\sqrt{n})$ bits information can be transmitted covertly and reliably from transmitters to receivers over n channel uses while the warden can achieve correct detections if the amount of transmitted information exceeds this square root law. Actually, this conclusion is pessimistic since the intrinsic uncertainty of wireless channels and the background noise are not taken into account in the considered communication systems of [7]. For example, [8] and [9] indicate that $O(n)$ bits information can be transmitted to the receiver when eavesdroppers don't exactly know the background noise power or the channel state information (CSI). Besides, existing works also resort to other uncertainties to enhance the performance of covert communications [10]–[12], [4]. In particular, a full-duplex receiver is adopted in [10] for generating power-varying artificial noise to obtain a decent covert rate. In [11], the random transmit power is leveraged to confuse the warden on the detection of covert transmissions. An uninformed jammer is introduced in [12] to assist covert communications by actively generating jamming signals under different channel models. Later in [4], a multi-jammer scheme with uncoordinated jammer selection is studied to defeat the warden. Considering more practical scenarios, [13] evaluates the influence of imperfect CSI on the system covert rate, and [14] explores the case with multiple randomly distributed wardens and maximize the average effective covert throughput by jointly optimizing the transmit power and blocklength.

The aforementioned works validate the effectiveness of the covert communication techniques from different perspectives, however, they only investigate the single-antenna covert communication scenarios. In fact, multi-antenna technologies

H. Xiao, X. Hu, P. Mu, W. Wang, and T.-X. Zheng are with the School of Information and Communication Engineering, Xi'an Jiaotong University, Xi'an 710049, China. (email: hanxiaonuli@stu.xjtu.edu.cn, xiaoyanhu@xjtu.edu.cn, {pcmu, wjwang, zhengtx}@mail.xjtu.edu.cn).

K.-K. Wong is with the Department of Electronic and Electrical Engineering, University College London, London WC1E 7JE, U.K. (email: kai-kit.wong@ucl.ac.uk)

K. Yang is with the School of Computer Science and Electronic Engineering, University of Essex, Colchester CO4 3SQ, U.K. (e-mail: kun-yang@essex.ac.uk).

are beneficial in improving the capacity and reliability of traditional wireless communications which are also conducive to enhancing the performance of covert communications [5], [15], [16]. Specifically, in [5], a multi-antenna transmitter and a full-duplex jamming receiver are utilized to alleviate the influence caused by the uncertainty of the warden. The authors in [15] study the potential performance gain of centralized and distributed multi-antenna transmitters in covert communication systems with random positions for wardens and interferers. Different from the above situations, a multi-antenna adversary warden is considered in [16] which indicates that a slight increase in the antenna number of the adversary warden will result in a dramatical fall of covert rate.

Although multi-antenna technologies can enhance covert-ness of communications through improving the ability of transmissions and receptions, it cannot tackle the issues brought by the randomness of wireless propagation environment. To break through this limitation, reconfigurable intelligent surface (RIS) has recently emerged as a promising solution [17]–[22]. In particular, RIS is usually a two-dimensional meta-material consisting of a large number of low-cost passive and adjustable reflecting elements. The electromagnetic properties (e.g., phase and amplitude) of the signals impinged on RIS can be adaptively adjusted with the assistance of RIS elements via a smart controller. Hence, the utilization of RISs is capable of reshaping desirable wireless propagation environment, which has attracted intensive attentions and been leveraged in many wireless communication scenarios including covert communications [19]–[22]. Specifically, [19] generally summarizes the application potentials of RIS in improving covert communications. Later in [20], the authors explore the performance gain of covert communications provided by RIS and first prove that the perfect covertness can be achieved with the aid of RIS when the instantaneous CSI of the warden is available. A multi-input multi-output (MIMO) covert communication system assisted by RIS is applied in [21] to resist the multi-antenna eavesdropper. Also, [22] investigates the RIS-assisted multi-antenna covert communications by jointly optimizing the active and passive beamformers.

B. Motivation and Contributions

It is worth noting that the RISs applied by the aforementioned works only reflect the incident signals which are limited to the scenarios that the transmitters and receivers locating at the same side of the RISs. However, in practical cases, users may be on either side of RIS, and thus the flexibility and effectiveness of conventional RIS appear inadequate in these cases. To overcome this limitation, a novel technology called simultaneously transmitting and reflecting RIS (STAR-RIS) is further emerged [23]. In particular, the incident signal will be separated into two parts when it arrives at the STAR-RIS, where one part is reflected to the same side of the incident signal and the other part is transited to the opposite side [24]. Note that STAR-RISs are capable of adjusting the reflected and transmitted signals by controlling the reflected and the transmitted coefficients simultaneously, which can help establish a more flexible full-space smart radio environment with 360° coverage. Therefore, STAR-RIS possesses a huge

application potential in wireless communications which has attracted intensive research interests from both academia and industry [23]. However, the investigation of leveraging STAR-RISs into wireless communication systems is still in its infancy stage. As for secure communication systems, only a small number of state-of-the-art works have utilized STAR-RISs to enhance the system secure performance [25], [26].

To our best knowledge, the application of STAR-RIS in covert communications has not been studied in existing works. This is the first work investigates a STAR-RIS assisted multi-antenna covert communication scenario so as to fully exploit the potentials of STAR-RIS in covert communications. Our main contributions are summarized as follows:

- **STAR-RIS-assisted Covert Communication Architecture:** A STAR-RIS-assisted covert communication architecture is constructed through which the legitimate users located on both sides of the STAR-RIS can be simultaneously served. Through elaborately design the reflected and transmitted coefficients of the STAR-RIS, this architecture can highly enhance the covert performance of the system though more flexible reconfigurations on the random wireless environment.
- **Closed-form Expressions for Covert System Indicators:** Based on the constructed covert communication system, The closed-form expressions of the minimum detection error probability (DEP) and the corresponding optimal detection threshold at the warden are analytically derived considering the worst-case scenario. Based on a lower bound of the detection threshold and the large system analytic techniques, we further derive a lower bound of the average minimum DEP which is leveraged to jointly design the active and passive beamformers. The reasonability for choosing this lower bound is further validated by simulation results.
- **Problem Formulation under Practical Constraints:** We formulate an optimization problem aiming at maximizing the covert rate of the considered STAR-RIS-assisted covert communication system, under the covert communication constraint and the quality of service (QoS) constraint based on communication outage analysis, by jointly optimizing the active and passive beamforming at the base station (BS) and STAR-RIS. Due to the strongly coupled optimization variables and the characteristic amplitude constraint introduced by STAR-RIS, it is challenging to solve the formulated problem directly.
- **Alternating Algorithm with Guaranteed Convergence:** An optimization algorithm based on alternating strategy is proposed to solve the formulated optimization problem in an iterative manner. In particular, the original problem is divided into three subproblems which are effectively solved by the semi-definite relaxation (SDR) method and Dinkelbach’s algorithm. It is verified that the convergence of the proposed algorithm can always been guaranteed.
- **Performance Improvement:** The effectiveness of the proposed algorithm is validated by numerical results where we evaluate the average covert rate of the considered STAR-RIS-assisted system in comparison with a benchmark using the conventional RIS and a baseline algorithm

called the globally convergent version of method of moving asymptotes (GCMMA). It is shown that the proposed algorithm can achieve great performance improvement compared with the baselines and the advantages are more obvious with a larger number of STAR-RIS elements.

The rest of this paper is organized as follows. In Section II, we introduce the STAR-RIS-aided covert communication system model. The DEP of the warden and communication outage probability based on this model are derived and analyzed in Section III. Section IV formulates the optimization problem and designs an iterative algorithm for jointly optimizing the passive and active beamforming. Section V shows the simulation results to validate the effectiveness of the proposed algorithm. Finally, a conclusion is drawn in Section VI

Notation: Operator \circ denotes the Hadamard product. $(\cdot)^T$, $(\cdot)^H$ and $(\cdot)^*$ represent transpose, conjugate transpose and conjugate, respectively. $\text{Diag}(\mathbf{a})$ denotes a diagonal matrix with diagonal elements in vector \mathbf{a} , $\text{diag}(\mathbf{A})$ denotes a vector whose elements are composed of the diagonal elements of matrix \mathbf{A} . $|\cdot|$ and $\|\cdot\|_2$ denote the complex modulus and the spectral norm, respectively. $\mathbb{C}^{N \times N}$ stands for the set of $N \times N$ complex matrices. $x \sim \mathcal{CN}(a, b)$ and $x \sim \exp(\lambda)$ denote the circularly symmetric complex Gaussian random variable with mean a and variance b and the exponential random variable with mean λ , respectively. $\text{Tr}(\cdot)$ represents the trace. $\mathbf{A} \succeq 0$ indicates that matrix \mathbf{A} is a positive semidefinite matrix. $\mathbf{1}_{N \times 1}$ represents the vector with $N \times 1$ entries that are 1.

II. SYSTEM MODEL

In this paper, we consider a STAR-RIS-assisted covert communication system model as shown in Fig.1, mainly consisting of a M -antenna BS transmitter (Alice) assisted by a STAR-RIS with N elements, a covert user (Bob) and a warden user (Willie) both equipped with a single antenna, and an assistant public user (Carol) with two antennas. Willie tries to detect the existence of data transmissions from Alice to Bob preparing for some security attacks. It is assumed that the single-antenna Bob and Willie work at the half-duplex mode, while the two-antenna Carol operates in the full-duplex mode where one antenna receives the transmitted signals from Alice and the other one transmits jamming signals to weaken Willie's detection ability. Due to the existence of blockages, we assume that there is no direct links between Alice and all the users, which is reasonable in practical environment. The STAR-RIS is deployed at the users' vicinity to enhance the end-to-end communications between Alice and the legal users Bob and Carol while confusing the detection of the warden user Willie. Without loss of generality, we consider a scenario that Bob and Carol locate on opposite sides of the STAR-RIS which can be served simultaneously by the reflected (T) and transmitted (R) signals via STAR-RIS, respectively.¹The energy splitting protocol is adopted for STAR-RIS whose all elements can work at T&R modes simultaneously [24].

The wireless communication channels from Alice to STAR-RIS, and from STAR-RIS to Bob, Carol, Willie are denoted as $\mathbf{H}_{\text{AR}} = \sqrt{l_{\text{AR}}}\mathbf{G}_{\text{AR}} \in \mathbb{C}^{N \times M}$ and $\mathbf{h}_{\text{rb}} = \sqrt{l_{\text{rb}}}\mathbf{g}_{\text{rb}} \in \mathbb{C}^{N \times 1}$,

¹Similar to [17] and [22], we ignore the signals reflected or transmitted more than once by the STAR-RIS considering the severe path losses.

$\mathbf{h}_{\text{rc}} = \sqrt{l_{\text{rc}}}\mathbf{g}_{\text{rc}} \in \mathbb{C}^{N \times 1}$, $\mathbf{h}_{\text{rw}} = \sqrt{l_{\text{rw}}}\mathbf{g}_{\text{rw}} \in \mathbb{C}^{N \times 1}$, respectively. In particular, \mathbf{G}_{AR} and \mathbf{g}_{rb} , \mathbf{g}_{rc} , \mathbf{g}_{rw} are the small-scale Rayleigh fading coefficients whose entries are independent identically distributed (i.i.d.) following the complex Gaussian distribution with zero mean and unit variance. In addition, l_{AR} and l_{rb} , l_{rc} , l_{rw} are the large-scale path loss coefficients modeled as $\sqrt{\frac{\rho_0}{d^\alpha}}$, where ρ_0 denotes the reference power gain at a distance of one meter (m), α represents the path-loss exponent, and d corresponds to the node distances of d_{AR} and d_{rb} , d_{rc} , d_{rw} . We assume that the considered STAR-RIS-assisted covert communication system operates in the time division duplex (TDD) mode, so that the uplink channel estimation techniques based on STAR-RIS can be exploited to estimate the aforementioned communication CSI by utilizing the channel reciprocity [27]. As for the full-duplex assistant user Carol, its self-interference channel can be modeled as $h_{\text{cc}} = \sqrt{\phi}g_{\text{cc}}$, where $g_{\text{cc}} \sim \mathcal{CN}(0, 1)$, $\phi \in [0, 1]$ is the self-interference cancellation (SIC) coefficient determined by the performing efficiency of the SIC [10], [28].

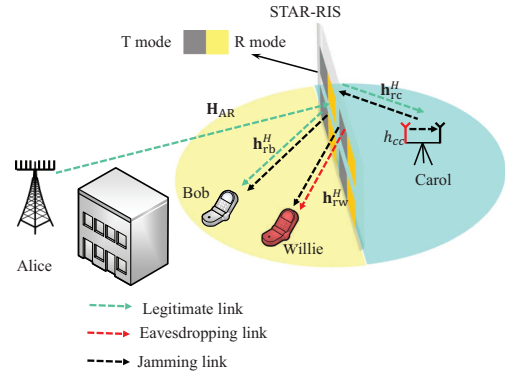


Fig. 1. System model for STAR-RIS-assisted covert communications.

In this paper, we assume that the instantaneous CSI between STAR-RIS and Alice, Bob, Carol (i.e., \mathbf{H}_{AR} , \mathbf{h}_{rb} , \mathbf{h}_{rc}) is available at Alice, while only the statistical CSI between STAR-RIS and the Willie (\mathbf{h}_{rw}) is known at Alice. In contrast, it is assumed that Willie is capable to know the instantaneous CSI of all the users, i.e., \mathbf{h}_{rw} , \mathbf{h}_{rb} and \mathbf{h}_{rc} , but can only access the statistical CSI of Alice, i.e., \mathbf{H}_{AR} . As for the jamming signals transmitted by Carol, we assume that the power of the jamming signals, denoted as P_j , follows the uniform distribution with P_j^{max} being the maximum power limit [10], [22]. It is assumed that Willie can only obtain the distribution of the jamming power, and thus it is difficult for Willie to detect the existence of communications between Alice and Bob under the random jamming interference.

Under such a covert strategy, the received signals at Bob and Carol in the considered STAR-RIS-assisted covert communication system can be respectively expressed as

$$y_b[k] = \mathbf{h}_{\text{rb}}^H \Theta_r \mathbf{H}_{\text{AR}} (\mathbf{w}_b s_b[k] + \mathbf{w}_c s_c[k]) + \mathbf{h}_{\text{rb}}^H \Theta_t \mathbf{h}_{\text{rc}}^* \sqrt{P_j} s_j[k] + n_b[k], \quad (1)$$

$$y_c[k] = \mathbf{h}_{\text{rc}}^H \Theta_t \mathbf{H}_{\text{AR}} (\mathbf{w}_b s_b[k] + \mathbf{w}_c s_c[k]) + h_{\text{cc}} \sqrt{P_j} s_j[k] + n_c[k], \quad (2)$$

where $k \in \mathcal{K} \triangleq \{1, \dots, K\}$ denotes the index of each communication channel use with the maximum number of K in a time slot. $\Theta_r = \text{Diag} \left\{ \sqrt{\beta_r^1} e^{j\phi_r^1}, \dots, \sqrt{\beta_r^N} e^{j\phi_r^N} \right\}$ and $\Theta_t = \text{Diag} \left\{ \sqrt{\beta_t^1} e^{j\phi_t^1}, \dots, \sqrt{\beta_t^N} e^{j\phi_t^N} \right\}$ respectively indicate the STAR-RIS reflected and transmitted coefficient matrices, where $\beta_r^n, \beta_t^n \in [0, 1]$, $\beta_r^n + \beta_t^n = 1$ and $\phi_r^n, \phi_t^n \in [0, 2\pi)$, for $\forall n \in \mathcal{N} \triangleq \{1, 2, \dots, N\}$. In addition, $\mathbf{w}_b \in \mathbb{C}^{M \times 1}$ and $\mathbf{w}_c \in \mathbb{C}^{M \times 1}$ are the precoding vectors at Alice for Bob and Carol, respectively. $s_b[k]$ and $s_c[k] \sim \mathcal{CN}(0, 1)$ are the signals transmitted by Alice to Bob and Carol while $s_j[k] \sim \mathcal{CN}(0, 1)$ is the jamming signal transmitted by Carol, where we try to hide the transmission of $s_b[k]$ from the detection of Willie. Also, we use $n_b[k] \sim \mathcal{CN}(0, \sigma_b^2)$ and $n_c[k] \sim \mathcal{CN}(0, \sigma_c^2)$ to represent the AWGN noise received at Bob and Carol with σ_b^2 and σ_c^2 being the corresponding noise power.²

Note that the instantaneous jamming power P_j and the self-interference channel h_{cc} of Carol are unavailable at Alice, thus the randomness introduced by P_j and h_{cc} is possible to incur communication outage. When the required communication rate from Alice to Bob (R_b) or Carol (R_c) exceeds the corresponding channel capacity (C_b, C_c), the communication outage occurs. Hence, the communication outage probability at Bob and Carol can be respectively expressed as

$$\delta_{AB} = \Pr(C_b < R_b), \quad (3)$$

$$\delta_{AC} = \Pr(C_c < R_c). \quad (4)$$

To guarantee the communication quality between Alice and Bob/Carol, the issue of communication outage also needs to be addressed in the considered covert communication system.

III. ANALYSIS ON STAR-RIS-ASSISTED COVERT COMMUNICATIONS

A. Covert Communication Detection Strategy at Willie

In this section, we detail the detection strategy of Willie for STAR-RIS-assisted covert communications from Alice to Bob. In particular, Willie attempts to judge whether there exists covert transmissions based on the received signal sequence $\{y_w[k]\}_{k \in \mathcal{K}}$ in a time slot. Thus, Willie has to face a binary hypothesis for detection, which includes a null hypothesis, \mathcal{H}_0 , representing that Alice only transmits public signals to Carol, and an alternative hypothesis, \mathcal{H}_1 , indicating that Alice transmits both public signals and covert signals to Carol and Bob, respectively. Furthermore, the received signals at Willie based on the two hypotheses are given by

$$\mathcal{H}_0 : y_w[k] = \mathbf{h}_{rw}^H \Theta_r \mathbf{H}_{AR} \mathbf{w}_c s_c[k] + \mathbf{h}_{rb}^H \Theta_t \mathbf{h}_{rc}^* \sqrt{P_j} s_j[k] + n_w[k], \quad k \in \mathcal{K}, \quad (5)$$

$$\mathcal{H}_1 : y_w[k] = \mathbf{h}_{rw}^H \Theta_r \mathbf{H}_{AR} \mathbf{w}_b s_b[k] + \mathbf{h}_{rw}^H \Theta_r \mathbf{H}_{AR} \mathbf{w}_c s_c[k] + \mathbf{h}_{rb}^H \Theta_t \mathbf{h}_{rc}^* \sqrt{P_j} s_j[k] + n_w[k], \quad k \in \mathcal{K}, \quad (6)$$

where $n_w[k] \sim \mathcal{CN}(0, \sigma_w^2)$ is the AWGN received at Willie. We assume that Willie utilizes a radiometer to detect the covert signals from Alice to Bob, owing to its properties of low complexity and ease of implementation [11], [29].

²It is worth noting that we ignore the jamming signals reflected by STAR-RIS at Carol mainly due to the fact that it is negligible compared with the self-interference jamming signals received by Carol.

According to the working mechanism of the radiometer, the average power of the received signals at Willie in a time slot, i.e., $\bar{P}_w = \frac{1}{K} \sum_{k=1}^K |y_w[k]|^2$, is employed for statistical test. Similar to the existing works, (e.g., [4], [10], [22]), we assume that Willie uses infinite number of signal samples to implement binary detection, i.e., $K \rightarrow \infty$. Hence, the average received power at Willie \bar{P}_w can be asymptotically approximated as (7) which is shown at the top of the next page. Willie needs to analyze \bar{P}_w to decide whether the communication between Alice and Bob is under the hypotheses of \mathcal{H}_0 or \mathcal{H}_1 , and its decision rule can be presented as

$$\bar{P}_w \underset{\mathcal{D}_0}{\overset{\mathcal{D}_1}{\gtrless}} \tau_{dt}, \quad (8)$$

where \mathcal{D}_0 (or \mathcal{D}_1) indicates the decision that Willie favors \mathcal{H}_0 (or \mathcal{H}_1), and $\tau_{dt} > 0$ is the corresponding detection threshold.

In this paper, we adopt the DEP as Willie's detection performance metric and consider the worst case scenario that Willie can optimize its detection threshold to obtain the minimum DEP. According to the Neyman-Pearson criterion, the minimum DEP of Willie is the likelihood ratio [12], [22], which can be expressed as

$$\Lambda(\mathbf{y}_w) = \frac{f_{\mathbf{y}_w|\mathcal{H}_1}(\mathbf{y}_w | \mathcal{H}_1)}{f_{\mathbf{y}_w|\mathcal{H}_0}(\mathbf{y}_w | \mathcal{H}_0)}, \quad (9)$$

where $\mathbf{y}_w = \{y_w[1], \dots, y_w[K]\}$ is Willie's received signal vector, $f_{\mathbf{y}_w|\mathcal{H}_0}$ and $f_{\mathbf{y}_w|\mathcal{H}_1}$ are the probability density functions (PDFs) of the sampling signals when \mathcal{H}_0 and \mathcal{H}_1 are true, respectively. However, it is difficult to derive the likelihood ratio due to the fact that the instantaneous CSI of \mathbf{H}_{AR} is unavailable at Willie, which introduces extra randomness in received signal \mathbf{y}_w .

To solve this problem, we will derive the false alarm (FA) probability and the miss detection (MD) probability to further obtain the minimum DEP. Specifically, FA probability represents the probability of Willie making the decision \mathcal{D}_1 under \mathcal{H}_0 , i.e., $P_{FA} = \Pr(\mathcal{D}_1 | \mathcal{H}_0)$, while MD probability is the probability of Willie making the decision \mathcal{D}_0 under \mathcal{H}_1 , i.e., $P_{MD} = \Pr(\mathcal{D}_0 | \mathcal{H}_1)$. Hence, the DEP of Willie can be written as

$$P_e = P_{FA} + P_{MD} = \Pr(\mathcal{D}_1 | \mathcal{H}_0) + \Pr(\mathcal{D}_0 | \mathcal{H}_1). \quad (10)$$

It is easy to note that $0 \leq P_e \leq 1$ where $P_e = 0$ indicates that Willie can always correctly detect the existence of the cover communications between Alice and Bob, while $P_e = 1$ means that Willie is never able to make correct detections. By choosing a reasonable detection threshold τ_{dt} , the minimum DEP denoted as P_e^* , can be obtained at Willie. Also, in order to achieve the covertness of communications, it is necessary to guarantee $P_e^* \geq 1 - \epsilon$, where $\epsilon \in (0, 1)$ is a quite small value required by the system performance indicators.

B. Analysis on Detection Error Probability

In this section, we first derive the analytical expressions for P_{FA} and P_{MD} in closed form, based on the distribution of \bar{P}_w under \mathcal{H}_0 and \mathcal{H}_1 . Then, the optimal detection threshold τ_{dt}^* and the minimum DEP P_e^* are obtained by analyzing the

$$\bar{P}_w = \lim_{K \rightarrow +\infty} \frac{1}{K} \sum_{k=1}^K |y_w[k]|^2 = \begin{cases} |\mathbf{h}_{rw}^H \Theta_r \mathbf{H}_{AR} \mathbf{w}_c|^2 + |\mathbf{h}_{rw}^H \Theta_t \mathbf{h}_{rc}^*|^2 P_j + \sigma_w^2, & \mathcal{H}_0, \\ |\mathbf{h}_{rw}^H \Theta_r \mathbf{H}_{AR} \mathbf{w}_b|^2 + |\mathbf{h}_{rw}^H \Theta_r \mathbf{H}_{AR} \mathbf{w}_c|^2 + |\mathbf{h}_{rw}^H \Theta_t \mathbf{h}_{rc}^*|^2 P_j + \sigma_w^2, & \mathcal{H}_1, \end{cases} \quad (7)$$

$$P_e = \begin{cases} 1, & \tau_{dt} < \sigma_w^2, \\ 1 + \frac{\tilde{\lambda} \left(e^{-\frac{\tau_{dt} - \sigma_w^2}{\lambda}} - 1 \right) - \lambda e^{-\frac{\tau_{dt} - \sigma_w^2}{\lambda}} + \lambda}{\gamma P_j^{\max}}, & \sigma_w^2 \leq \tau_{dt} < \sigma_w^2 + \gamma P_j^{\max}, \\ 1 + \frac{\tilde{\lambda} e^{-\frac{\tau_{dt} - \sigma_w^2}{\lambda}} \left(1 - e^{\frac{\gamma P_j^{\max}}{\lambda}} \right) + \lambda e^{-\frac{\tau_{dt} - \sigma_w^2}{\lambda}} \left(e^{\frac{\gamma P_j^{\max}}{\lambda}} - 1 \right)}{\gamma P_j^{\max}}, & \tau_{dt} \geq \gamma P_j^{\max} + \sigma_w^2, \end{cases} \quad (13)$$

analytical expression of DEP. Considering the fact that the instantaneous CSI of channel \mathbf{h}_{rw} is not available at Alice, thus we derive a lower bound for the average the minimum DEP over \mathbf{h}_{rw} . In particular, the analytical expressions for P_{FA} and P_{MD} can be obtained through Theorem 1.

Theorem 1. *The analytical expressions for FA probability P_{FA} and MD probability P_{MD} are respectively given as*

$$P_{FA} = \begin{cases} 1, & \tau_{dt} < \sigma_w^2, \\ 1 - \frac{(\tau_{dt} - \sigma_w^2) + \lambda e^{-\frac{\tau_{dt} - \sigma_w^2}{\lambda}} - \lambda}{\gamma P_j^{\max}}, & \sigma_w^2 \leq \tau_{dt} < \sigma_w^2 + \gamma P_j^{\max}, \\ \frac{e^{-\frac{\tau_{dt} - \sigma_w^2}{\lambda}} \left(e^{\frac{\gamma P_j^{\max}}{\lambda}} - 1 \right) \lambda}{\gamma P_j^{\max}}, & \tau_{dt} \geq \sigma_w^2 + \gamma P_j^{\max}, \end{cases} \quad (11)$$

$$P_{MD} = \begin{cases} 0, & \tau_{dt} < \sigma_w^2, \\ \frac{(\tau_{dt} - \sigma_w^2) + \tilde{\lambda} e^{-\frac{\tau_{dt} - \sigma_w^2}{\lambda}} - \tilde{\lambda}}{\gamma P_j^{\max}}, & \sigma_w^2 \leq \tau_{dt} < \sigma_w^2 + \gamma P_j^{\max}, \\ 1 - \frac{e^{-\frac{\tau_{dt} - \sigma_w^2}{\lambda}} \left(e^{\frac{\gamma P_j^{\max}}{\lambda}} - 1 \right) \tilde{\lambda}}{\gamma P_j^{\max}}, & \tau_{dt} \geq \gamma P_j^{\max} + \sigma_w^2, \end{cases} \quad (12)$$

which are shown in closed form with $\lambda = \|\mathbf{h}_{rw}^H \Theta_r\|_2^2 \mathbf{w}_c^H \mathbf{w}_c$, $\tilde{\lambda} = \|\mathbf{h}_{rw}^H \Theta_r\|_2^2 (\mathbf{w}_b^H \mathbf{w}_b + \mathbf{w}_c^H \mathbf{w}_c)$, and $\gamma = |\mathbf{h}_{rw}^H \Theta_t \mathbf{h}_{rc}^*|^2$.

Proof. The proof is given in Appendix A. \square

According to (11) and (12), we find that σ_w^2 and $\sigma_w^2 + \gamma P_j^{\max}$ are two important boundaries affecting the values of P_{FA} and P_{MD} . Specifically, when $\tau_{dt} \leq \sigma_w^2$, complete FAs will be performed by Willie and the MDs can be totally avoided. Furthermore, with the increase of detection threshold τ_{dt} from σ_w^2 to $+\infty$, P_{FA} will experience a decrease from 1 to 0, while P_{MD} will have an opposite trend. Based on the analytical expressions of (11) and (12), the analytical closed-form expressions of DEP can be given as (13) which is shown at the top of the next page.

It is important to point out that we consider the worst case scenario that Willie can optimize its detection threshold to minimize the DEP. Here, the closed-form solution of the optimal τ_{dt}^* is provided in the following theorem.

Theorem 2. *The optimal detection threshold τ_{dt}^* to minimize the DEP of Willie in the considered STAR-RIS-assisted communication system is given by*

$$\tau_{dt}^* = \frac{\tilde{\lambda} \lambda}{\lambda - \tilde{\lambda}} \ln \Delta + \sigma_w^2 \in [\sigma_w^2 + \gamma P_j^{\max}, \infty), \quad (14)$$

where $\Delta = \frac{e^{\frac{\gamma P_j^{\max}}{\lambda}} - 1}{e^{\frac{\tilde{\lambda} \lambda}{\lambda - \tilde{\lambda}} - 1}}$ is a function of λ , $\tilde{\lambda}$ and γ .

Proof. The proof is given in Appendix B. \square

Substituting (14) into (13) and adopting some algebraic manipulations, the analytical closed-form expression of the minimum DEP can be obtained as

$$P_e^* = 1 - \frac{\tilde{\lambda} \left(e^{\frac{\gamma P_j^{\max}}{\lambda}} - 1 \right) (\Delta)^{\frac{\lambda}{\lambda - \tilde{\lambda}}} - \lambda \left(e^{\frac{\gamma P_j^{\max}}{\lambda}} - 1 \right) (\Delta)^{\frac{\tilde{\lambda}}{\lambda - \tilde{\lambda}}}}{\gamma P_j^{\max}}. \quad (15)$$

Since Alice only knows the statistical CSI of channel \mathbf{h}_{rw} , the average minimum DEP over \mathbf{h}_{rw} , denoted as $\bar{P}_e^* = \mathbb{E}_{\mathbf{h}_{rw}}(P_e^*)$, is usually utilized to evaluate the covert communications between Alice and Bob [5], [29]. In (15), λ , $\tilde{\lambda}$ and γ are all random variables including \mathbf{h}_{rw} , and thus they are coupled to each other, which makes it challenging to calculate the \bar{P}_e^* directly. To solve this problem, large system analytic techniques are utilized to remove the couplings among λ , $\tilde{\lambda}$ and γ , which are widely adopted to analyze the performance limitation of wireless communication systems (e.g., [22], [30]–[33]). By assuming that the STAR-RIS is equipped with a large number of low-cost elements, then we can obtain the asymptotic analytic result of P_e^* . In particular, we first apply the large system analytic technique on λ , then the asymptotic equality about λ can be given as

$$\begin{aligned} \lim_{N \rightarrow \infty} \frac{\|\mathbf{h}_{rw}^H \Theta_r\|_2^2 \varpi_c}{N} &= \lim_{N \rightarrow \infty} \frac{\mathbf{h}_{rw}^H \Theta_r \Theta_r^H \mathbf{h}_{rw} \varpi_c}{N} \\ &\stackrel{(a)}{\rightarrow} \frac{l_{rw} \varpi_c}{N} \text{tr} \left(\Theta_r \Theta_r^H \right) \\ &= \frac{l_{rw} \varpi_c}{N} \theta_r = \frac{\lambda_a}{N}, \end{aligned} \quad (16)$$

where the convergence (a) is due to [30, Corollary 1]. Here, $\varpi_c = \mathbf{w}_c^H \mathbf{w}_c$, $\theta_r = \text{diag}(\Theta_r)^H \text{diag}(\Theta_r)$, and $\lambda_a = l_{rw} \varpi_c \theta_r$

is the asymptotic result of λ . Similarly, the asymptotic result of $\tilde{\lambda}$ can be expressed as

$$\tilde{\lambda}_a = l_{rw}\theta_r(\varpi_b + \varpi_c), \quad (17)$$

where we define $\varpi_b = \mathbf{w}_b^H \mathbf{w}_b$.

With the results of λ_a and $\tilde{\lambda}_a$ based on the large system analytic technique, the uncertainty of λ and $\tilde{\lambda}$ can be removed from the perspective of Alice. Substituting λ_a and $\tilde{\lambda}_a$ into (15), we obtain the asymptotic analytical result of the minimum DEP P_{ea}^* with respect to (w.r.t.) the random variable γ

$$P_{ea}^* = 1 - \frac{l_{rw}\theta_r\varpi_b}{\gamma P_j^{\max}} (\Delta(\gamma))^{\frac{-\varpi_c}{\varpi_b}} \left(e^{\frac{\gamma P_j^{\max}}{l_{rw}\theta_r(\varpi_b + \varpi_c)}} - 1 \right). \quad (18)$$

It is easy to verify that $\gamma = |\mathbf{h}_{rw}^H \Theta_t \mathbf{h}_{rc}^*|^2 \sim \exp(\lambda_{rw})$ where $\lambda_{rw} = \|\Theta_t \mathbf{h}_{rc}^*\|_2^2$. By averaging P_{ea}^* over γ , we can get the average asymptotic analytical result of the minimum DEP as

$$\begin{aligned} \bar{P}_{ea}^* &= \mathbb{E}_\gamma (P_{ea}^*) \\ &= \int_0^{+\infty} \left(1 - \frac{l_{rw}\theta_r\varpi_b}{\gamma P_j^{\max}} (\Delta(\gamma))^{\frac{-\varpi_c}{\varpi_b}} \right. \\ &\quad \left. \left(e^{\frac{\gamma P_j^{\max}}{l_{rw}\theta_r(\varpi_b + \varpi_c)}} - 1 \right) \right) \times \frac{1}{\lambda_{rw}} e^{-\frac{\gamma}{\lambda_{rw}}} d\gamma. \end{aligned} \quad (19)$$

Due to the existence of $\Delta(\gamma)$ in P_{ea}^* , the integral in (19) for calculating \bar{P}_{ea}^* over the random variable γ is non-integrable. Therefore, the exact analytical expression for \bar{P}_{ea}^* is mathematically intractable. In order to guarantee the covert constraint $\bar{P}_{ea}^* \geq 1 - \epsilon$ always holds, we further adopt a lower bound of \bar{P}_{ea}^* to evaluate the covertness of communications.

Specifically, we use a lower bound $\hat{\Delta}(\gamma) \triangleq e^{\gamma P_j^{\max} \left(\frac{\lambda_a - \lambda_a}{\lambda_a \lambda_a} \right)}$ to replace $\Delta(\gamma)$. It is easy to demonstrate that $\Delta(\gamma) > \hat{\Delta}(\gamma)$ always holds when $\gamma \in (0, +\infty)$, and the relative gap between these two variables gradually goes to zero with the increase of γ .³ Replacing the $\Delta(\gamma)$ in (19) with $\hat{\Delta}(\gamma)$, we can get a lower bound of \bar{P}_{ea}^* given by

$$\begin{aligned} \hat{P}_{ea}^* &\triangleq \int_0^{+\infty} \left(1 - \frac{l_{rw}\theta_r\varpi_b}{\gamma P_j^{\max}} (\hat{\Delta}(\gamma))^{\frac{-\varpi_c}{\varpi_b}} \right. \\ &\quad \left. \left(e^{\frac{\gamma P_j^{\max}}{l_{rw}\theta_r(\varpi_b + \varpi_c)}} - 1 \right) \right) \times \frac{1}{\lambda_{rw}} e^{-\frac{\gamma}{\lambda_{rw}}} d\gamma \\ &= 1 + \frac{l_{rw}\theta_r\varpi_b \left(\ln \frac{l_{rw}\theta_r(\varpi_b + \varpi_c)}{l_{rw}\theta_r(\varpi_b + \varpi_c) + P_j^{\max}\lambda_{rw}} \right)}{P_j^{\max}\lambda_{rw}} < \bar{P}_{ea}^*. \end{aligned} \quad (20)$$

Therefore, in the following sections, $\hat{P}_{ea}^* \geq 1 - \epsilon$ will be leveraged as a tighter covert constraint to jointly design the active and passive beamforming variables of the system.

C. Analysis on Communication Outage Probability

As we mentioned before, the randomness introduced by the jamming signal power P_j and the self-interference channel h_{cc} of Carol is possible to result in communication outages between Alice and Bob/Carol. In order to guarantee the QoS of

communications, the communication outage constraints should be taken into consideration.

It is known that the channel capacity at Bob and Carol can be respectively written as

$$C_b = \log_2 \left(1 + \frac{|\mathbf{h}_{rb}^H \Theta_r \mathbf{H}_{AR} \mathbf{w}_b|^2}{|\mathbf{h}_{rb}^H \Theta_r \mathbf{H}_{AR} \mathbf{w}_c|^2 + |\mathbf{h}_{rb}^H \Theta_t \mathbf{h}_{rc}^*|^2 P_j + \sigma_b^2} \right), \quad (21)$$

$$C_c = \log_2 \left(1 + \frac{|\mathbf{h}_{rc}^H \Theta_t \mathbf{H}_{AR} \mathbf{w}_c|^2}{|\mathbf{h}_{rc}^H \Theta_t \mathbf{H}_{AR} \mathbf{w}_b|^2 + |h_{cc}|^2 P_j + \sigma_c^2} \right). \quad (22)$$

Hence, when the required transmission rate between Alice and Bob (or Carol) is selected as R_b (or R_c), the closed-form expressions of the communication outage probabilities at Bob and Carol can be obtained through Theorem 3.

Theorem 3. *The communication outage probabilities between Alice and Bob/Carol are respectively derived as*

$$\delta_{AB} = \begin{cases} 0, & \Upsilon > P_j^{\max}, \\ 1 - \frac{\Upsilon}{P_j^{\max}}, & 0 \leq \Upsilon \leq P_j^{\max}, \\ 1, & \Upsilon < 0, \end{cases} \quad (23)$$

$$\delta_{AC} = \begin{cases} e^{-\frac{\Gamma}{\phi P_j^{\max}}} + \frac{\Gamma}{\phi P_j^{\max}} \text{Ei} \left(-\frac{\Gamma}{\phi P_j^{\max}} \right), & \Gamma \geq 0, \\ 1, & \Gamma < 0, \end{cases} \quad (24)$$

where $\Upsilon = \frac{|\mathbf{h}_{rb}^H \Theta_r \mathbf{H}_{AR} \mathbf{w}_b|^2 - (2^{R_b} - 1)(|\mathbf{h}_{rb}^H \Theta_r \mathbf{H}_{AR} \mathbf{w}_c|^2 + \sigma_b^2)}{(2^{R_b} - 1)|\mathbf{h}_{rb}^H \Theta_t \mathbf{h}_{rc}^*|^2}$ and $\Gamma = \frac{|\mathbf{h}_{rc}^H \Theta_t \mathbf{H}_{AR} \mathbf{w}_c|^2 - (2^{R_c} - 1)(|\mathbf{h}_{rc}^H \Theta_t \mathbf{H}_{AR} \mathbf{w}_b|^2 + \sigma_c^2)}{(2^{R_c} - 1)}$. Here, $\text{Ei}(\cdot)$ is the exponential integral function given by

$$\text{Ei}(x) = - \int_{-x}^{\infty} \frac{e^{-t}}{t} dt. \quad (25)$$

Proof. The proof is given in Appendix C. \square

The communication outage constraints are then defined as $\delta_{AB} \leq \iota$ and $\delta_{AC} \leq \kappa$ where ι and κ are two communication outage thresholds required by the system performance indicators for Bob and Carol, respectively. In this paper, we try to maximize the covert rate of Bob under the covert constraint $\hat{P}_{ea}^* \geq 1 - \epsilon$ and the communication outage constraints. It is easy to note that δ_{AB} and δ_{AC} are segment functions with uncertain segment points Υ and Γ determined by the active and passive beamforming variables, i.e., \mathbf{w}_b , \mathbf{w}_c and Θ_r , Θ_t , which will be jointly optimized in the next section. Hence, it is difficult to handle the two communication outage constraints in an optimization problem. In order to facilitate the optimization and analysis of the considered problem, we equivalently re-express the two communication outage constraints as

$$\Upsilon \geq P_j^{\max}(1 - \iota) \iff R_b \leq R_{bb}, \quad (26)$$

$$\Gamma \geq \sigma^* \iff R_c \leq R_{cc}, \quad (27)$$

where σ^* is the solution to the equation of $\delta_{AC} = \kappa$ which can be numerically solved by the bi-section search method. In addition, R_{bb} and R_{cc} are respectively the upper bounds

³The reasonability about the selection of $\hat{\Delta}(\gamma)$ (or \hat{P}_{ea}^*) will be further verified based on the simulation results.

of R_b and R_c in order to guarantee the two communication outage constraints which can be expressed as

$$R_{bb} = \log_2 \left(1 + \frac{|\mathbf{h}_{rb}^H \Theta_r \mathbf{H}_{AR} \mathbf{w}_b|^2}{|\mathbf{h}_{rb}^H \Theta_r \mathbf{H}_{AR} \mathbf{w}_c|^2 + |\mathbf{h}_{rb}^H \Theta_t \mathbf{h}_{rc}^*|^2 P_j^{\max} (1 - \iota) + \sigma_b^2} \right), \quad (28)$$

$$R_{cc} = \log_2 \left(1 + \frac{|\mathbf{h}_{rc}^H \Theta_t \mathbf{H}_{AR} \mathbf{w}_c|^2}{|\mathbf{h}_{rc}^H \Theta_t \mathbf{H}_{AR} \mathbf{w}_b|^2 + \sigma^* + \sigma_c^2} \right). \quad (29)$$

Base on the above analysis, we know that the maximum covert rate for Bob under the communication outage constraint is R_{bb} , then we can maximize R_{bb} accordingly to improve the system covert performance. Similarly, the maximum communication rate for Carol under the communication outage constraint is R_{cc} , and we introduce a constraint $R_{cc} \geq R^*$ to guarantee the QoS for the assistant user Carol where R^* is a minimum required communication rate for Carol.

IV. PROBLEM FORMULATION AND ALGORITHM DESIGN

A. Optimization Problem Formulation

On the basis of the previous discussions in section III, we formulate the optimization problem in this section. Specifically, we will maximize the covert rate between Alice and Bob under the covert communication constraint while ensuring the QoS at Carol with the QoS constraint, by jointly optimizing the active and passive beamforming variables, i.e., \mathbf{w}_b , \mathbf{w}_c and Θ_r , Θ_t . Hence, the optimized problem is formulated as

$$\max_{\Theta_r, \Theta_t, \mathbf{w}_b, \mathbf{w}_c} R_{bb}, \quad (30a)$$

$$\text{s.t. } \|\mathbf{w}_b\|_2^2 + \|\mathbf{w}_c\|_2^2 \leq P_{\max} \quad (30a)$$

$$\frac{l_{rw} \theta_r \varpi_b \ln \left(\frac{l_{rw} \theta_r (\varpi_b + \varpi_c)}{l_{rw} \theta_r (\varpi_b + \varpi_c) + P_j^{\max} \lambda_{rw}} \right)}{P_j^{\max} \lambda_{rw}} \geq -\epsilon, \quad (30b)$$

$$R_{cc} \geq R^*, \quad (30c)$$

$$\beta_r^n + \beta_t^n = 1, \quad (30d)$$

$$\phi_r^n, \phi_t^n \in [0, 2\pi). \quad (30e)$$

where (30a) is the transmission power constraint for Alice with P_{\max} being the maximum transmitted power; (30b) is an equivalent covert communication constraint of $\hat{P}_{ea}^* \geq 1 - \epsilon$; (30c) represents the QoS constraint for Carol; (30d) and (30e) are the amplitude and phase shift constraints for STAR-RIS, respectively. Actually, it is challenging to solve the formulated optimization problem because of the following reasons. Firstly, the active and passive beamforming variables, \mathbf{w}_b , \mathbf{w}_c and Θ_r , Θ_t are strongly coupled in the objective function, covert communication constraint (30b) and QoS constraint (30c). In addition, the utilization of STAR-RIS introduces a characteristic amplitude constraint (30d) due to the fact that Θ_r and Θ_t depend on each other in terms of element amplitudes.

Hence, the traditional convex optimization algorithms cannot be used directly to solve the non-convex optimized problem (30). To tackle this issue, the alternating strategy is leveraged to design the optimization algorithm. Specifically,

we first divide the original problem into three subproblems where two subproblems are focused on designing the active beamformer variables \mathbf{w}_b , \mathbf{w}_c , while the passive beamformer variables Θ_r , Θ_t are obtained by solving the last subproblem. After the convergence of the algorithm, we can finally obtain the solution for joint active and passive beamforming.

B. Active Beamforming Design

In this section, we formulate two subproblems based on the original problem (30) which are solved to design the active beamforming variables \mathbf{w}_b and \mathbf{w}_c , respectively.

1) *Active Beamforming Design for \mathbf{w}_b* : First, we consider the active beamforming design for \mathbf{w}_b with given \mathbf{w}_c and the passive beamforming variables Θ_r , Θ_t . In this circumstance, the objective function of the original problem turns into maximizing $|\mathbf{h}_{rb}^H \Theta_r \mathbf{H}_{AR} \mathbf{w}_b|^2$, and the QoS constraint (30c) is equivalent to $|\mathbf{h}_{rc}^H \Theta_t \mathbf{H}_{AR} \mathbf{w}_b|^2 \leq f(R^*)$ with $f(R^*) = \frac{|\vartheta_t^T (\mathbf{h}_{rc}^* \circ \mathbf{H}_{AR}) \mathbf{w}_c|^2}{2^{R^*} - 1} - \sigma^* - \sigma_c^2$. Hence, the corresponding subproblem can be formulated as

$$\max_{\mathbf{w}_b} \left| \vartheta_r^T \mathbf{H}_{rb}^* \mathbf{H}_{AR} \mathbf{w}_b \right|^2, \quad (31a)$$

$$\text{s.t. } \|\mathbf{w}_b\|_2^2 \leq P_{\max} - \|\mathbf{w}_c\|_2^2, \quad (31a)$$

$$\frac{l_{rw} \theta_r \varpi_b \ln \left(1 + \frac{P_j^{\max} \lambda_{rw}}{l_{rw} \theta_r (\varpi_b + \varpi_c)} \right)}{P_j^{\max} \lambda_{rw}} \leq \epsilon, \quad (31b)$$

$$\left| \vartheta_t^T \mathbf{H}_{rc}^* \mathbf{H}_{AR} \mathbf{w}_b \right|^2 \leq f(R^*). \quad (31c)$$

Here, it is easy to verify that

$$\mathbf{h}_{rb}^H \Theta_r \mathbf{H}_{AR} = \vartheta_r^T \mathbf{H}_{rb}^* \mathbf{H}_{AR}, \quad (32)$$

$$\mathbf{h}_{rc}^H \Theta_t \mathbf{H}_{AR} = \vartheta_t^T \mathbf{H}_{rc}^* \mathbf{H}_{AR}, \quad (33)$$

by vectorizing the diagonal matrixes Θ_r and Θ_t as $\vartheta_r = \text{diag}(\Theta_r)$ and $\vartheta_t = \text{diag}(\Theta_t)$, and matrixing the vectors \mathbf{h}_{rb} and \mathbf{h}_{rc} as $\mathbf{H}_{rb} = \text{Diag}(\mathbf{h}_{rb})$ and $\mathbf{H}_{rc} = \text{Diag}(\mathbf{h}_{rc})$. It is worth noting that the optimization problem (31) is still non-convex due to the non-concave objective function and the non-convex covert communication constraint (31b) recalling that $\varpi_b = \mathbf{w}_b^H \mathbf{w}_b$.

To effectively address the non-convex problem (31), we resort to the SDR method [34]. In particular, let $\mathbf{W}_b = \mathbf{w}_b \mathbf{w}_b^H$, then problem (31) can be equivalently transformed as

$$\max_{\mathbf{W}_b} \text{Tr}(\mathbf{A} \mathbf{W}_b), \quad (34a)$$

$$\text{s.t. } \text{Tr}(\mathbf{W}_b) \leq P_{\max} - \|\mathbf{w}_c\|_2^2, \quad (34a)$$

$$\varpi_b \ln \left(1 + \frac{P_j^{\max} \lambda_{rw}}{l_{rw} \theta_r (\varpi_b + \varpi_c)} \right) \leq \frac{\epsilon P_j^{\max} \lambda_{rw}}{l_{rw} \theta_r}, \quad (34b)$$

$$\text{Tr}(\mathbf{B} \mathbf{W}_b) \leq f(R^*), \quad (34c)$$

$$\mathbf{W}_b \succeq \mathbf{0}, \quad (34d)$$

$$\text{rank}(\mathbf{W}_b) = 1, \quad (34e)$$

where $\mathbf{A} = (\mathbf{H}_{rb}^* \mathbf{H}_{AR})^H \vartheta_r^* \vartheta_r^T (\mathbf{H}_{rb}^* \mathbf{H}_{AR})$, $\mathbf{B} = (\mathbf{H}_{rc}^* \mathbf{H}_{AR})^H \vartheta_t^* \vartheta_t^T (\mathbf{H}_{rc}^* \mathbf{H}_{AR})$. Although (34b) is still a non-convex constraint about \mathbf{W}_b , we note that the left-side of (34b), denoted as $g(\varpi_b)$, is a concave function of $\varpi_b = \text{Tr}(\mathbf{W}_b)$. Thus, the first-order Taylor expansion of $g(\varpi_b)$ can be leveraged

$$\frac{\partial g}{\partial \varpi_b}(\varpi_b^{(m)}) = \ln \left(1 + \frac{P_j^{\max} \lambda_{rw}}{l_{rw} \theta_r (\varpi_b^{(m)} + \varpi_c)} \right) + \frac{-\varpi_b^{(m)} l_{rw} \theta_r P_j^{\max} \lambda_{rw}}{(\varpi_b^{(m)} + \varpi_c) (l_{rw} \theta_r (\varpi_b^{(m)} + \varpi_c) + P_j^{\max} \lambda_{rw})}, \quad (36)$$

to replace it iteratively, which is an upper-bound linear approximation and generate a tighter convex substitute for (34b). Specifically, in the $(m+1)$ -th iteration of the overall proposed algorithm ($m = 0, 1, \dots$), the first-order Taylor expansion of $g(\varpi_b)$, with the given point $\varpi_b^{(m)}$ obtained in the m -th iteration, can be expressed as

$$\hat{g}(\varpi_b, \varpi_b^{(m)}) = g(\varpi_b^{(m)}) + \frac{\partial g}{\partial \varpi_b}(\varpi_b^{(m)}) * (\varpi_b - \varpi_b^{(m)}), \quad (35)$$

where $\frac{\partial g}{\partial \varpi_b}(\varpi_b^{(m)})$ is given by (36) at the top of the next page.

Therefore, the problem (34) in the $(m+1)$ -th iteration can be reformulated as

$$\begin{aligned} \max_{\mathbf{W}_b} \text{Tr}(\mathbf{A}\mathbf{W}_b), \\ \text{s.t. } \hat{g}(\varpi_b, \varpi_b^{(m)}) \leq \frac{\epsilon P_j^{\max} \lambda_{rw}}{l_{rw} \theta_r}, \end{aligned} \quad (37a)$$

$$(34a), (34c), (34d), (34e). \quad (37b)$$

Note that the remaining non-convexity of problem (37) is the non-convex rank-one constraint (34e). To tackle this issue, we employ the SDR techniques to remove this constraint, and then problem (37) can be transformed into a standard convex semidefinite programming (SDP) problem which is able to be effectively solved by existing convex optimization solvers such as CVX [35]. As stated in [34], [36], there is a relatively high probability that the obtained optimal SDP solution cannot satisfy the rank-one constraint, i.e., $\text{rank}(\mathbf{W}_b) \neq 1$. Thus, it is necessary to implement additional steps to construct the rank-one solution from the obtained higher-rank solution, through the commonly used eigenvector approximation or Gaussian randomization methods [34], [37].

2) *Active Beamforming Design for \mathbf{w}_c* : On the other hand, for given \mathbf{w}_b , Θ_r and Θ_t , the original optimization problem (30) can be simplified as

$$\begin{aligned} \min_{\mathbf{w}_c} \left| \boldsymbol{\vartheta}_r^T \mathbf{H}_{rb}^* \mathbf{H}_{AR} \mathbf{w}_c \right|^2, \\ \text{s.t. } \|\mathbf{w}_c\|_2^2 \leq P_{\max} - \|\mathbf{w}_b\|_2^2, \end{aligned} \quad (38a)$$

$$\varpi_c \leq C(\epsilon), \quad (38b)$$

$$\left| \boldsymbol{\vartheta}_t^T \mathbf{H}_{rc}^* \mathbf{H}_{AR} \mathbf{w}_c \right|^2 \geq \hat{f}(R^*), \quad (38c)$$

where $C(\epsilon) = \frac{P_j^{\max} \lambda_{rw}}{l_{rw} \theta_r \left(e^{\frac{\epsilon P_j^{\max} \lambda_{rw}}{l_{rw} \theta_r \varpi_b} - 1} \right)} - \varpi_b$, $\hat{f}(R^*) = (2^{R^*} -$

1) $\left(\left| \boldsymbol{\vartheta}_t^T \mathbf{H}_{rc}^* \mathbf{H}_{AR} \mathbf{w}_b \right|^2 + \sigma^* + \sigma_c^2 \right)$, and $\varpi_c = \mathbf{w}_c^H \mathbf{w}_c$.

Similarly, we leverage the SDR method to handle the non-convex optimized problem (38). By defining $\mathbf{W}_c = \mathbf{w}_c \mathbf{w}_c^H$,

the problem can be transformed as

$$\min_{\mathbf{W}_c} \text{Tr}(\mathbf{A}\mathbf{W}_c),$$

$$\text{s.t. } \text{Tr}(\mathbf{W}_c) \leq P_{\max} - \|\mathbf{w}_b\|_2^2, \quad (39a)$$

$$\text{Tr}(\mathbf{W}_c) \leq C(\epsilon), \quad (39b)$$

$$\text{Tr}(\mathbf{B}\mathbf{W}_c) \geq \hat{f}(R^*), \quad (39c)$$

$$\text{rank}(\mathbf{W}_c) = 1, \quad (39d)$$

$$\mathbf{W}_c \succeq \mathbf{0}. \quad (39e)$$

The problem (39) can be optimally solved by removing the rank-one constraint (39d), and then the rank-one solution can be constructed through the existing approaches.

C. Joint Passive Beamforming Design for STAR-RIS

After the active beamforming design, we can optimize the passive beamforming variables $\boldsymbol{\vartheta}_r$ and $\boldsymbol{\vartheta}_t$, with \mathbf{w}_b and \mathbf{w}_c being fixed as the obtained solutions in the previous subsection. On the basis of the original problem (30), the corresponding optimization problem for joint passive beamforming for STAR-RIS design can be expressed as

$$\begin{aligned} \max_{\boldsymbol{\vartheta}_r, \boldsymbol{\vartheta}_t} \gamma_{bb}(\boldsymbol{\vartheta}_r, \boldsymbol{\vartheta}_t), \\ \text{s.t. } \frac{l_{rw} \theta_r \varpi_b \ln \left(1 + \frac{P_j^{\max} \lambda_{rw}}{l_{rw} \theta_r (\varpi_b + \varpi_c)} \right)}{P_j^{\max} \lambda_{rw}} \leq \epsilon, \end{aligned} \quad (40a)$$

$$\tilde{f}(\boldsymbol{\vartheta}_t) \geq 0, \quad (40b)$$

$$\beta_r^n + \beta_t^n = 1, \quad (40c)$$

$$\phi_r^n, \phi_t^n \in [0, 2\pi), \quad (40d)$$

where

$$\begin{aligned} \gamma_{bb} &= \frac{|\mathbf{h}_{rb}^H \Theta_r \mathbf{H}_{AR} \mathbf{w}_b|^2}{|\mathbf{h}_{rb}^H \Theta_r \mathbf{H}_{AR} \mathbf{w}_c|^2 + |\mathbf{h}_{rb}^H \Theta_t \mathbf{h}_{rc}^*|^2 P_j^{\max} (1 - \iota) + \sigma_b^2}, \\ &= \frac{\boldsymbol{\vartheta}_r^T \mathbf{C} \boldsymbol{\vartheta}_r^*}{\boldsymbol{\vartheta}_r^T \mathbf{D} \boldsymbol{\vartheta}_r^* + \boldsymbol{\vartheta}_t^T \mathbf{E} \boldsymbol{\vartheta}_t^* P_j^{\max} (1 - \iota) + \sigma_b^2}, \end{aligned} \quad (41)$$

$$\mathbf{C} = (\mathbf{H}_{rb}^* \mathbf{H}_{AR}) \mathbf{w}_b \mathbf{w}_b^H (\mathbf{H}_{rb}^* \mathbf{H}_{AR})^H, \quad (42)$$

$$\mathbf{D} = (\mathbf{H}_{rb}^* \mathbf{H}_{AR}) \mathbf{w}_c \mathbf{w}_c^H (\mathbf{H}_{rb}^* \mathbf{H}_{AR})^H, \quad (43)$$

$$\mathbf{E} = (\mathbf{H}_{rb}^* \mathbf{H}_{rc}^*) (\mathbf{H}_{rb}^* \mathbf{H}_{rc}^*)^H, \quad (44)$$

$$\begin{aligned} \tilde{f}(\boldsymbol{\vartheta}_t) &= \left| \boldsymbol{\vartheta}_t^T \mathbf{H}_{rc}^* \mathbf{H}_{AR} \mathbf{w}_c \right|^2 - (2^{R^*} - 1) \times \\ &\quad \left(\left| \boldsymbol{\vartheta}_t^T \mathbf{H}_{rc}^* \mathbf{H}_{AR} \mathbf{w}_b \right|^2 + \sigma^* + \sigma_c^2 \right). \end{aligned} \quad (45)$$

We can find that the fractional objective function and the constraints (40a), (40b) in problem (40) are non-convex w.r.t. $\boldsymbol{\vartheta}_r$ and $\boldsymbol{\vartheta}_t$ recalling that $\theta_r = \text{diag}(\Theta_r)^H \text{diag}(\Theta_r) = \boldsymbol{\vartheta}_r^H \boldsymbol{\vartheta}_r$ and $\lambda_{rw} = \|\Theta_t \mathbf{h}_{rc}^*\|_2^2 = \|\boldsymbol{\vartheta}_t \circ \mathbf{h}_{rc}^*\|_2^2$, which makes this problem difficult to be solved directly.

In order to effectively solve the optimization problem (40), we first adopt the Dinkelbach's algorithm [38, Chapter3.2.1] and the SDR techniques to deal with the objective function. In the $(i+1)$ -th iteration of the Dinkelbach's algorithm, the objective function can be transformed as

$$\widehat{\gamma}_{\text{bb}}^{(i+1)}(\mathbf{Q}_r, \mathbf{Q}_t) = \text{Tr}(\mathbf{C}\mathbf{Q}_r) - \chi^{(i)} \left(\text{Tr}(\mathbf{D}\mathbf{Q}_r) + \text{Tr}(\mathbf{E}\mathbf{Q}_t) P_j^{\max}(1 - \iota) + \sigma_b^2 \right), \quad (46)$$

where $\mathbf{Q}_r = \boldsymbol{\vartheta}_r^* \boldsymbol{\vartheta}_r^T$ and $\mathbf{Q}_t = \boldsymbol{\vartheta}_t^* \boldsymbol{\vartheta}_t^T$ will be optimized to obtain the reflection and transmission coefficients of STAR-RIS. In addition, the parameter $\chi^{(i)}$ is updated with

$$\chi^{(i)} = \frac{\text{Tr}(\mathbf{C}\mathbf{Q}_r^{(i)})}{\left(\text{Tr}(\mathbf{D}\mathbf{Q}_r^{(i)}) + \text{Tr}(\mathbf{E}\mathbf{Q}_t^{(i)}) P_j^{\max}(1 - \iota) + \sigma_b^2 \right)}, \quad (47)$$

where $\mathbf{Q}_r^{(i)}$ and $\mathbf{Q}_t^{(i)}$ are the optimized solution through the i -th iteration. In this way, the objective function has been transformed into an affine function w.r.t. \mathbf{Q}_r and \mathbf{Q}_t .

Next, we try to deal with the constraints in problem (40). For the left-side of covert communication constraint (40a), we find that it is a monotonically decreasing function of $\frac{\lambda_{\text{rw}}}{\theta_r}$. Thus, the constraint (40a) can be equivalently rewritten as

$$\frac{\lambda_{\text{rw}}}{\theta_r} \geq \varphi(\epsilon), \quad (48)$$

where $\varphi(\epsilon)$ can be numerically obtained by employing the bisection search method. According to the expressions of λ_{rw} and θ_r , they can be reformulated as

$$\lambda_{\text{rw}} = \boldsymbol{\beta}_t^T (\mathbf{h}_{\text{rc}} \circ \mathbf{h}_{\text{rc}}^*), \quad \theta_r = \boldsymbol{\beta}_r^T \mathbf{I}_{N \times 1}. \quad (49)$$

where $\boldsymbol{\beta}_r = [\beta_r^1, \dots, \beta_r^N]^T$, $\boldsymbol{\beta}_t = [\beta_t^1, \dots, \beta_t^N]^T$.

Similarly, by using SDR techniques, the equivalent form of $\tilde{f}(\boldsymbol{\vartheta}_t)$ in constraint (40b) w.r.t. \mathbf{Q}_t can be derived as

$$\tilde{f}(\mathbf{Q}_t) = \text{Tr}(\mathbf{F}\mathbf{Q}_t) - (2^{R^*} - 1) (\text{Tr}(\mathbf{G}\mathbf{Q}_t) + \sigma^* + \sigma_c^2), \quad (50)$$

where we have

$$\mathbf{F} = (\mathbf{H}_{\text{rc}}^* \mathbf{H}_{\text{AR}}) \mathbf{w}_c \mathbf{w}_c^H (\mathbf{H}_{\text{rc}}^* \mathbf{H}_{\text{AR}})^H, \quad (51a)$$

$$\mathbf{G} = (\mathbf{H}_{\text{rc}}^* \mathbf{H}_{\text{AR}}) \mathbf{w}_b \mathbf{w}_b^H (\mathbf{H}_{\text{rc}}^* \mathbf{H}_{\text{AR}})^H. \quad (51b)$$

Based on the above analysis, the optimization problem (40) in the $(i+1)$ -th iteration can be formulated as

$$\begin{aligned} & \max_{\mathbf{Q}_r, \mathbf{Q}_t, \boldsymbol{\beta}_r, \boldsymbol{\beta}_t} \widehat{\gamma}_{\text{bb}}^{(i+1)}(\mathbf{Q}_r, \mathbf{Q}_t), \\ & \text{s.t.} \quad \frac{\boldsymbol{\beta}_t^T (\mathbf{h}_{\text{rc}} \circ \mathbf{h}_{\text{rc}}^*)}{\boldsymbol{\beta}_r^T \mathbf{I}_{N \times 1}} \geq \varphi(\epsilon), \end{aligned} \quad (52a)$$

$$\tilde{f}(\mathbf{Q}_t) \geq 0, \quad (52b)$$

$$\beta_r^n + \beta_t^n = 1, \quad (52c)$$

$$\text{diag}(\mathbf{Q}_r) = \boldsymbol{\beta}_r, \text{diag}(\mathbf{Q}_t) = \boldsymbol{\beta}_t, \quad (52d)$$

$$\text{rank}(\mathbf{Q}_r) = 1, \text{rank}(\mathbf{Q}_t) = 1, \quad (52e)$$

$$\mathbf{Q}_r \succeq 0, \mathbf{Q}_t \succeq 0. \quad (52f)$$

However, problem (52) is still a non-convex optimization problem due to the two rank-one constraints in (52e). Due to the dependence of \mathbf{Q}_r and \mathbf{Q}_t , it is difficult to re-construct the rank-one solution if we remove the rank-one constraints

directly. To handle this issue, we equivalently rewrite the rank-one constraints as [18]

$$\text{rank}(\mathbf{Q}_r) = 1 \iff \eta_r \triangleq \text{Tr}(\mathbf{Q}_r) - \|\mathbf{Q}_r\|_2 = 0, \quad (53a)$$

$$\text{rank}(\mathbf{Q}_t) = 1 \iff \eta_t \triangleq \text{Tr}(\mathbf{Q}_t) - \|\mathbf{Q}_t\|_2 = 0, \quad (53b)$$

where $\|\mathbf{Q}\|_2$ represents the spectral norm which is a convex function of \mathbf{Q} . Note that for any positive semidefinite matrix $\mathbf{Q} \succeq 0$, the inequality $\text{Tr}(\mathbf{Q}) - \|\mathbf{Q}\|_2 \geq 0$ always holds and the equality is satisfied if and only if $\text{rank}(\mathbf{Q}) = 1$. Based on the non-negative feature of η_r and η_t , we add them into the objective function of problem (52) as penalty terms for the rank-one constraints. Hence, the optimization problem can be re-expressed as

$$\begin{aligned} & \max_{\mathbf{Q}_r, \mathbf{Q}_t, \boldsymbol{\beta}_r, \boldsymbol{\beta}_t} \widehat{\gamma}_{\text{bb}}^{(i+1)}(\mathbf{Q}_r, \mathbf{Q}_t) - \rho_1 \eta_r - \rho_2 \eta_t, \\ & \text{s.t.} \quad \frac{\boldsymbol{\beta}_t^T (\mathbf{h}_{\text{rc}} \circ \mathbf{h}_{\text{rc}}^*)}{\boldsymbol{\beta}_r^T \mathbf{I}_{N \times 1}} \geq \varphi(\epsilon), \end{aligned} \quad (54a)$$

$$(52b), (52c), (52d), (52f), \quad (54b)$$

where $\rho_1, \rho_2 > 0$ are the introduced penalty coefficients. Now, the optimization problem (54) is still non-convex because of the non-convexity of the penalty terms η_r and η_t . By replacing the convex spectral norms in η_r and η_t with their linear lower-bound, i.e., first-order Taylor expansions, we can obtain the upper-bound linear approximations for η_r and η_t as

$$\begin{aligned} \eta_r & \leq \text{Tr}(\mathbf{Q}_r) - \left(\|\mathbf{Q}_r^{(i)}\|_2 + \text{Tr} \left(\mathbf{q}_r^{(i)} (\mathbf{q}_r^{(i)})^H (\mathbf{Q}_r - \mathbf{Q}_r^{(i)}) \right) \right) \\ & = \widehat{\eta}_r(\mathbf{Q}_r), \end{aligned} \quad (55)$$

$$\begin{aligned} \eta_t & \leq \text{Tr}(\mathbf{Q}_t) - \left(\|\mathbf{Q}_t^{(i)}\|_2 + \text{Tr} \left(\mathbf{q}_t^{(i)} (\mathbf{q}_t^{(i)})^H (\mathbf{Q}_t - \mathbf{Q}_t^{(i)}) \right) \right) \\ & = \widehat{\eta}_t(\mathbf{Q}_t), \end{aligned} \quad (56)$$

where $\mathbf{q}_r^{(i)}$ and $\mathbf{q}_t^{(i)}$ are the eigenvectors corresponding to the largest eigenvalues of $\mathbf{Q}_r^{(i)}$ and $\mathbf{Q}_t^{(i)}$. Hence, $\widehat{\gamma}_{\text{bb}}^{(i+1)}(\mathbf{Q}_r, \mathbf{Q}_t) - \rho_1 \widehat{\eta}_r(\mathbf{Q}_r) - \rho_2 \widehat{\eta}_t(\mathbf{Q}_t)$ is a linear lower-bound of the objective function in problem (54), which will be further utilized as the objective function in problem (54) to obtain the solution of \mathbf{Q}_r and \mathbf{Q}_t in the $(i+1)$ -th iteration, denoted $\mathbf{Q}_r^{(i+1)}$ and $\mathbf{Q}_t^{(i+1)}$.

In conclusion, to solve the optimization problem (40) for joint passive beamforming design, we propose a two-tier iterative algorithm as summarized in Algorithm 1, where the outer loop is for updating the penalty coefficients ρ_1 and ρ_2 through the penalty method [39] and the inner loop is for updating \mathbf{Q}_r and \mathbf{Q}_t through the Dinkelbach's algorithm [38], [40]. Here, $\omega > 1$ is the scaling factor of the penalty coefficient. Also, $v_1 > 0$ denotes the penalty violation and $v_2 > 0$ indicates the gap of the objective functions between two adjacent iterations of the Dinkelbach's algorithm, which are given by

$$v_1 = \max\{\eta_r, \eta_t\}, \quad (57)$$

$$v_2 = \left| \widehat{\gamma}_{\text{bb}}^{(i+1)}(\mathbf{Q}_r^{(i+1)}, \mathbf{Q}_t^{(i+1)}) - \widehat{\gamma}_{\text{bb}}^{(i)}(\mathbf{Q}_r^{(i)}, \mathbf{Q}_t^{(i)}) \right|. \quad (58)$$

Algorithm 1: Proposed Iterative Algorithm for Problem (40) on Joint Passive Beamforming Design of STAR-RIS

- 1: Initialize feasible point $(\mathbf{Q}_r^{(0)}, \mathbf{Q}_t^{(0)})$, penalty coefficients $(\rho_1^{(0)}, \rho_2^{(0)})$, and calculate v_1 ; Define the accuracy tolerance thresholds $\varepsilon_1, \varepsilon_2$; Set iteration index $l = 0$ for outer loop.
 - 2: **While** $v_1 > \varepsilon_1$ or $l = 0$ **do**
 - 3: Initialize $\chi^{(0)}$ and set $i = 0$ for inner loop.
 - 4: **While** $v_2 > \varepsilon_2$ or $i = 0$ **do**
 - 5: Solve the problem (54) with given $(\mathbf{Q}_r^{(i)}, \mathbf{Q}_t^{(i)})$.
 - 6: Update the $(\mathbf{Q}_r^{(i+1)}, \mathbf{Q}_t^{(i+1)})$ with obtained solution.
 - 7: Calculate $v_2, \chi^{(i+1)}$ based on the obtained solution, and let $i = i + 1$.
 - 8: **end while**
 - 9: Calculate v_1 ; Update $\rho_1^{(l+1)} = \omega \rho_1^{(l)}, \rho_2^{(l+1)} = \omega \rho_2^{(l)}$; Let $(\mathbf{Q}_r^{(0)}, \mathbf{Q}_t^{(0)}) = (\mathbf{Q}_r^{(i)}, \mathbf{Q}_t^{(i)})$ and $l = l + 1$.
 - 10: **end while**
 - 11: Calculate the Θ_r, Θ_t through the obtained $\mathbf{Q}_r, \mathbf{Q}_t$.
-

D. Proposed Optimization Algorithm & Analysis on Complexity and Convergence

Algorithm 2 concludes the overall processes for solving the original optimization problem (30) for STAR-RIS-assisted covert communications, which is an alternating optimization algorithm to solve three subproblems alternatively as detailed in Section IV. Here, $v > 0$ represents the gap of objective values between two adjacent iterations, and the algorithm converges when v is below a predefined accuracy threshold ε .

Next, we give the analysis on the computational complexity of the proposed Algorithm 2. Specifically, the main complexity comes from solving the standard SDP subproblems⁴. In terms of active beamforming design for Alice, the computational complexity on solving the subproblems (34) and (39) can be respectively calculated as $\mathcal{O}(M^{3.5})$ and $\mathcal{O}(M^{3.5})$. For Algorithm 1 on joint passive beamforming design of STAR-RIS, the main complexity lies on solving the subproblem (54) which is dominated by $\mathcal{O}(2N^{3.5})$. Besides, we use the bisection search method to find $\varphi(\epsilon)$ in (48) with the complexity of $\mathcal{O}(\log_2(\frac{s_0}{\epsilon_t}))$ where s_0 and ϵ_t denote the length of the initial search interval and the accuracy tolerance, respectively. Hence, the computational complexity of Algorithm 1 is $\mathcal{O}(I_2 I_3 (2N^{3.5}) + \log_2(\frac{s_0}{\epsilon_t}))$, where I_2 and I_3 are the number of outer and inner iterations. Based on the above analysis, the computational complexity of the proposed alternating Algorithm 2 for solving the original covert communication problem (30) is dominated by $\mathcal{O}(I_1 (2M^{3.5} + \log_2(\frac{s_0}{\epsilon_t}) + I_2 I_3 (2N^{3.5})))$, where I_1 denotes the total iteration number of the proposed algorithm. The complexity is mainly determined by the number of antennas at Alice (M) and elements at STAR-RIS (N).

It is easy to verify that the convergence of the alternating Algorithm 2. For each iteration of Algorithm 2, we can always find a solution not worse than that of the previous iteration, considering the SDR and the Dinkelbach's algorithm leveraged

for solving the subproblems. Hence, the the objective function of problem (30) monotonically non-decreases w.r.t. the iteration index, and the algorithm finally converges subject to the transmit power limitation (30a), which will be further verified by simulation results.

Algorithm 2: Proposed Alternating Algorithm for STAR-RIS-assisted Covert Communications Problem (30)

- 1: Initialize feasible point $(\mathbf{w}_b^{(0)}, \mathbf{w}_c^{(0)}, \Theta_r^{(0)}, \Theta_t^{(0)})$; Define the tolerance accuracy ε ; Set iteration index $m = 0$.
 - 2: **While** $v > \varepsilon$ or $m = 0$ **do**
 - 3: Solve the relaxed version of the subproblem (34) with SDR method and use Gaussian randomization method to construct the rank-one solution, then update the \mathbf{w}_b .
 - 4: Similarly, solve the relaxed version of the subproblem (39) with SDR method and update the \mathbf{w}_c .
 - 5: Solve subproblem (40) with Algorithm 1 and update the Θ_r and Θ_t .
 - 6: Calculate the objective value $R_{\text{bb}}^{(m+1)}$ value and update $v = |R_{\text{bb}}^{(m+1)} - R_{\text{bb}}^{(m)}|^2$; Let $m = m + 1$.
 - 7: **end while**
-

V. SIMULATION RESULTS

In this section, we show the numerical simulation results to verify the effectiveness of the proposed STAR-RIS-assisted covert communication scheme implemented by the proposed optimization Algorithm 2. Specifically, all the simulation results are averaged over 1000 independent channels realizations. For large-scale path loss coefficients, we assume $\rho_0 = -20\text{dB}$, $\alpha = 2.6$ and the distances are set as $d_{\text{AR}} = 500\text{m}$, $d_{\text{rb}} = 100\text{m}$, $d_{\text{rw}} = 80\text{m}$ and $d_{\text{rc}} = 150\text{m}$. Furthermore, we define the noise power $\sigma_b^2 = -140\text{ dBm}$, $\sigma_c^2 = -140\text{ dBm}$ and the self-interference coefficient $\phi = -160\text{ dB}$ [42]. In the proposed algorithm, the accuracy tolerance parameters ε , ε_1 and ε_2 are set as 10^{-4} , 10^{-8} and 10^{-8} , respectively.

To highlight the advantage of covert communication aided by STAR-RIS, we consider a baseline scheme which employs two adjacent conventional RISs to replace STAR-RIS where one is the reflection-only RIS and the other one is transmission-only RIS. The number of elements in these two RISs is selected as $N/2$ so as to achieve a fair comparison. We call this baseline scheme as "RIS-aided scheme". In addition, to further validate the effectiveness of the proposed algorithm, a general optimization method called GCMMA is adopted as a comparison algorithm to solve the problem [43], [44], which requires lower computational complexity and is capable of converging to the Karush-Kuhn-Tucker (KKT) solution.

In Fig. 2, we show the performance of average covert rate versus the transmitted power P_{max} at Alice, considering different QoS (R^*) and covert (ϵ) requirements. Specifically, we can find that the achievable covert rates for all schemes in all scenarios gradually increase with the growth of P_{max} before it reaching 6 dBW. And then the covert rates approach saturation when P_{max} further increases due to limitations of system settings. It is obvious that a significant performance improvement can be achieved by the proposed optimization scheme in

⁴For convex problems, we assume that the Interior point method is adopted and then calculate the computational complexity accordingly [41].

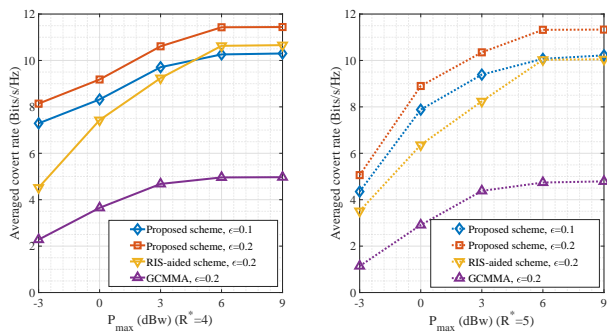


Fig. 2. Average covert rate versus the maximum transmit power P_{\max} of Alice with $P_j^{\max} = 0$ dBw, $M = 3$, $N = 30$, $\iota = 0.1$, $\kappa = 0.1$, and different ϵ and R^* .

comparison with the GCMMA method, which clearly validates the effectiveness of the proposed algorithm. Compared with the RIS-aided baseline scheme, we can find that the proposed STAR-RIS-assisted scheme possesses a strong superiority in enhancing the system covert performance, and the advantage may further expanded when with relaxed QoS requirement but limited transmit power budget (smaller R^* and P_{\max}). In addition, we can observe that a lower covert rate is achieved if the QoS or the covertness constraint becomes tighter, i.e., from $R^* = 4$ to $R^* = 5$, or from $\epsilon^* = 0.2$ to $\epsilon^* = 0.1$, which coincides with our intuition. Compared with the RIS-aided scheme, the performance degradation of proposed STAR-RIS assisted scheme with a moderate P_{\max} is much less serious.

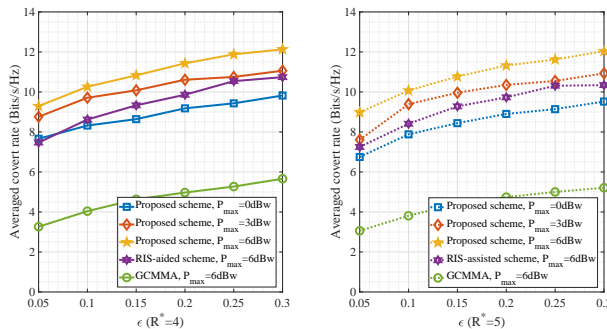


Fig. 3. Average covert rate versus the covert requirement ϵ with $P_j^{\max} = 0$ dBw, $M = 3$, $N = 30$, $\iota = 0.1$, $\kappa = 0.1$, and different P_{\max} and R^* .

Next in Fig. 3, we investigate the influence of the covert requirement, i.e., ϵ , on the performance of average covert rate, considering different P_{\max} and QoS requirements. In particular, $P_{\max} = 6$ dBw is selected to operate the RIS-aided baseline scheme for an evident comparison, and obvious performance improvement can be achieved by the proposed scheme. Even if a lower transmitted power budget, i.e., 3 dBw, is utilized, the proposed scheme can still obtain better performance. This is because the STAR-RIS possesses a more flexible regulation ability compared with the conventional RIS, which can adjust the element phases and amplitudes for both reflection and transmission. It can be seen that the proposed scheme highly outperforms the GCMMA algorithm and the performance gap enlarges with the increase of ϵ , indicating that the proposed scheme can achieve a much better solution

than the KKT solution converged by the GAMMA method.

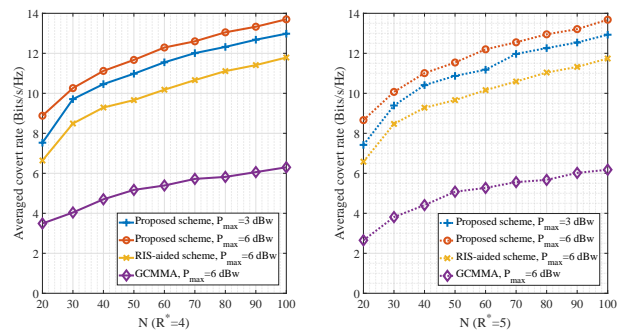


Fig. 4. Average covert rate versus the number of elements in STAR-RIS with $P_j^{\max} = 0$ dBw, $M = 3$, $\epsilon = 0.1$, $\iota = 0.1$, $\kappa = 0.1$, and different P_{\max} and R^* .

We present the variation curves of average covert rate w.r.t. the number of elements on STAR-RIS (N) in Fig. 4, under different transmit power P_{\max} and QoS constraints R^* . It can be observed that the average covert rates of all the schemes grow with N , since the increased elements can provide higher freedom degree for reconfiguration of propagation environment. However, the increasing rates gradually decrease with the growth of N , and this may due to the limitations of other system settings. Similarly, $P_{\max} = 6$ dBw is chosen to implement the two benchmark schemes, i.e., the RIS-aided and the GCMMA schemes. The obtained results further verify the advantages of the proposed STAR-RIS-assisted scheme which can achieve even better performance than the benchmark schemes in the scenario with a much smaller transmit power budget ($P_{\max} = 3$ dBw). In addition, the performance enhancement for the proposed scheme is more obvious as the number of elements becomes larger.

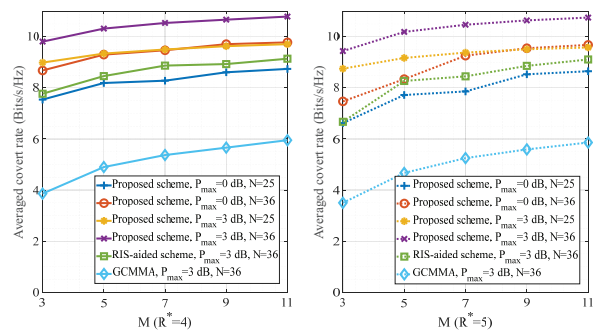


Fig. 5. Averaged covert rate versus the number of elements equipped at Alice with $P_j^{\max} = 0$ dBw, $\epsilon = 0.1$, $\iota = 0.1$, $\kappa = 0.1$, and different P_{\max} , N and R^* .

In Fig. 5, we explore the effects of the number of antennas equipped at the transmitter, i.e., M , on the available covert rate, considering different transmitted power P_{\max} , number of elements in STAR-RIS (N), and QoS requirements (R^*). In particular, with the growth of M , the average covert rates of all schemes gradually increase, but the increasing rates have downward trends. Besides, we can observe that higher transmitted power or more elements at STAR-RIS contribute to breaking the performance bottleneck imposed by channel characteristics and the number of antennas at Alice. Similarly,

evident performance gaps exist between the proposed scheme and the RIS-aided scheme even for the proposed scheme with a lower P_{\max} or fewer N . Compare with the GCMMA method, the proposed algorithm can still achieve better solutions in both scenarios with $R^* = 4$ and $R^* = 5$.

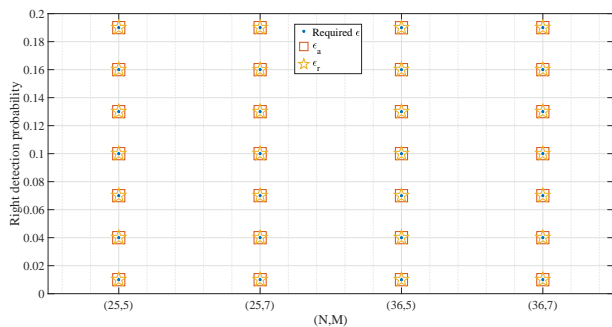


Fig. 6. Verifying the reasonability of choosing the lower bound of the minimum average DEP i.e., \hat{P}_{ea}^* , with $P_j^{\max} = 0$ dBW, $P_{\max} = 3$ dBW, $\iota = 0.1$, $\kappa = 0.1$, and different N and M .

Fig. 6 verifies the reasonability of adopting the lower bound of the minimum average DEP, i.e., \hat{P}_{ea}^* , to replace itself \bar{P}_{ea}^* , under different covertness requirements (ϵ), number of antennas at Alice (M), and elements equipped at RIS (N). In particular, we utilize the solution obtained by choosing the lower bound \hat{P}_{ea}^* to compute the accurate maximum average correct detection probability at Willie, which denotes ϵ_r . Note that $\epsilon_a = 1 - \hat{P}_{ea}^*$ represents the upper bound of ϵ_r . According to the obtained results, we can find that the lower bound in (20) is tight because ϵ_r and ϵ_a are almost identical in all considered scenarios with different covert requirements and different communication system configurations.

VI. CONCLUSIONS

In this work, we initially investigate the application potentials of STAR-RIS in covert communications. In particular, the closed-form expression of the minimum DEP about the STAR-RIS-aided covert communication system is analytically derived. And then we jointly design the active and passive beamforming at the BS and STAR-RIS, to maximize the covert rate taking into account of the minimum DEP of Willie and the communication outage probability experienced at Bob and Carol. Due to the strong coupling between active and

passive beamforming variables and the characteristic amplitude constraint introduced by the STAR-RIS, the proposed optimization problem is a non-convex problem. To effectively solve this covert communication problem, we elaborately design an alternating algorithm based on the SDR method and Dinkelbach's algorithm. Simulation results demonstrate that the STAR-RIS-assisted covert communication scheme highly outperforms the conventional RIS-aided scheme. In addition, the proposed iterative algorithm can effectively solve the formulated problem with guaranteed convergence.

APPENDIX A

PROOF OF THEOREM 1

To facilitate the analysis, we denote $\varrho_1 \triangleq \mathbf{h}_{\text{rw}}^H \Theta_r \mathbf{H}_{\text{AR}} \mathbf{w}_c$, and it is easy to demonstrate that ϱ_1 follows the complex Gaussian distribution with mean zero and variance $\lambda = \|\mathbf{h}_{\text{rw}}^H \Theta_r\|_2^2 \mathbf{w}_c^H \mathbf{w}_c$. Hence, the PDF of $|\varrho_1|^2$ can be written $f_{|\varrho_1|^2}(x) = \frac{e^{-\frac{x}{\lambda}}}{\lambda}$. In addition, we know that P_j follows the uniform distribution, and thus the analytical expression of the FA probability P_{FA} can be derived as (59), which is shown at the bottom of this page. Similarly, we can derive the MD probability P_{MD} as (12).

APPENDIX B

PROOF OF THEOREM 2

According to the analytical expression of DEP at Willie, i.e., P_e given in (13), we can see that P_e is a segment function based on the detection threshold τ_{dt} in three different ranges. Let us discuss the optimal detection τ_{dt}^* threshold in three ranges, respectively.

1) $\tau_{\text{dt}} < \sigma_w^2$: It is easy to note that $P_e = 1$ when $\tau_{\text{dt}} < \sigma_w^2$, indicating that Willie is always unable to distinguish the existence of communications between Alice and Bob. Hence, there is no need to optimize τ_{dt} to minimize the DEP when τ_{dt} falls into this range.

2) $\sigma_w^2 \leq \tau_{\text{dt}} < \sigma_w^2 + \gamma P_j^{\max}$: The first-order derivative of P_e w.r.t. τ_{dt} in this range is given by

$$\frac{\partial P_e}{\partial \tau_{\text{dt}}} = \frac{e^{-\frac{\tau_{\text{dt}} - \sigma_w^2}{\lambda}} - e^{-\frac{\tau_{\text{dt}} - \sigma_w^2}{\lambda}}}{\gamma P_j^{\max}}, \quad (60)$$

from which can find that $\frac{\partial P_e}{\partial \tau_{\text{dt}}} < 0$ always holds. Therefore, P_e decrease monotonically versus $\tau_{\text{dt}} \in [\sigma_w^2, \sigma_w^2 + \gamma P_j^{\max})$ and the optimal detection threshold is $\tau_{\text{dt}}^* = \sigma_w^2 + \gamma P_j^{\max}$.

$$\begin{aligned} P_{\text{FA}} &= \Pr(\bar{P}_w > \tau_{\text{dt}} | \mathcal{H}_0) \\ &= \begin{cases} 1, & \tau_{\text{dt}} < \sigma_w^2, \\ \int_0^\infty \frac{e^{-\frac{x}{\lambda}}}{\lambda} dx - \int_0^{\tau_{\text{dt}} - \sigma_w^2} \int_0^{\tau_{\text{dt}} - \sigma_w^2 - x} \frac{e^{-\frac{x}{\lambda}}}{\lambda} \frac{1}{\gamma P_j^{\max}} dy dx, & \sigma_w^2 \leq \tau_{\text{dt}} < \sigma_w^2 + \gamma P_j^{\max}, \\ \int_0^{\gamma P_j^{\max}} \int_{\tau_{\text{dt}} - \sigma_w^2 - y}^\infty \frac{e^{-\frac{x}{\lambda}}}{\lambda} \frac{1}{\gamma P_j^{\max}} dx dy, & \tau_{\text{dt}} \geq \gamma P_j^{\max} + \sigma_w^2, \end{cases} \\ &= \begin{cases} 1, & \tau_{\text{dt}} < \sigma_w^2, \\ 1 - \frac{(\tau_{\text{dt}} - \sigma_w^2) + \lambda e^{-\frac{\tau_{\text{dt}} - \sigma_w^2}{\lambda}} - \lambda}{\gamma P_j^{\max}}, & \sigma_w^2 \leq \tau_{\text{dt}} < \sigma_w^2 + \gamma P_j^{\max}, \\ \frac{e^{-\frac{\tau_{\text{dt}} - \sigma_w^2}{\lambda}} \left(e^{\frac{\gamma P_j^{\max}}{\lambda}} - 1 \right) \lambda}{\gamma P_j^{\max}}, & \tau_{\text{dt}} \geq \gamma P_j^{\max} + \sigma_w^2, \end{cases} \quad (59) \end{aligned}$$

3) $\tau_{dt} \geq \sigma_w^2 + \gamma P_j^{\max}$: We can further obtain the first-order derivative of P_e w.r.t. τ_{dt} in this range as

$$\frac{\partial P_e}{\partial \tau_{dt}} = \frac{e^{-\frac{\tau_{dt} - \sigma_w^2}{\lambda}} \left(e^{\frac{\gamma P_j^{\max}}{\lambda}} - 1 \right) + e^{-\frac{\tau_{dt} - \sigma_w^2}{\lambda}} \left(1 - e^{\frac{\gamma P_j^{\max}}{\lambda}} \right)}{\gamma P_j^{\max}} \quad (61)$$

Let $\frac{\partial P_e}{\partial \tau_{dt}} = 0$, we can obtain the unique solution of τ_{dt} in this range, i.e., $\tau_{dt} = \frac{\tilde{\lambda}\lambda}{\lambda - \tilde{\lambda}} \ln \Delta + \sigma_w^2 \in [\sigma_w^2 + \gamma P_j^{\max}, +\infty)$

where $\Delta = \frac{e^{\frac{\gamma P_j^{\max}}{\lambda}} - 1}{e^{\frac{\gamma P_j^{\max}}{\lambda}} - 1}$. It is easy to prove that P_e first decreases and then increases versus τ_{dt} in this range with $\frac{\tilde{\lambda}\lambda}{\lambda - \tilde{\lambda}} \ln \Delta + \sigma_w^2$ as the the inflection point. Hence, the optimal detection threshold for minimizing P_e is given as $\tau_{dt}^* = \frac{\tilde{\lambda}\lambda}{\lambda - \tilde{\lambda}} \ln \Delta + \sigma_w^2$.

Based on the above analysis, the optimal detection threshold τ_{dt}^* can be finally expressed as

$$\tau_{dt}^* = \begin{cases} \sigma_w^2 + \gamma P_j^{\max}, & \sigma_w^2 \leq \tau_{dt} < \sigma_w^2 + \gamma P_j^{\max}, \\ \frac{\tilde{\lambda}\lambda}{\lambda - \tilde{\lambda}} \ln \Delta + \sigma_w^2, & \tau_{dt} \geq \gamma P_j^{\max} + \sigma_w^2. \end{cases} \quad (62)$$

We can verify that P_e in (13) is a continuous segment function at the segment points σ_w^2 and $\sigma_w^2 + \gamma P_j^{\max}$. Therefore, the optimal detection threshold in the overall defined region for minimizing the DEP P_e is $\tau_{dt}^* = \frac{\tilde{\lambda}\lambda}{\lambda - \tilde{\lambda}} \ln \Delta + \sigma_w^2$.

APPENDIX C

PROOF OF THEOREM 3

When the required transmission rate between Alice and Bob is chosen as R_b , the communication outage probability at Bob under the randomness of the jamming power P_j can be calculated as

$$\begin{aligned} \delta_{AB} &= \Pr(C_b < R_b) \\ &= \Pr(P_j > \Upsilon) \\ &= \begin{cases} 1, & \Upsilon < 0, \\ \int_{\Upsilon}^{P_j^{\max}} \frac{1}{P_j} dy, & 0 \leq \Upsilon < P_j^{\max}, \\ 0, & \Upsilon \geq P_j^{\max}, \end{cases} \\ &= \begin{cases} 1, & \Upsilon < 0, \\ 1 - \frac{\Upsilon}{P_j^{\max}}, & 0 \leq \Upsilon < P_j^{\max}, \\ 0, & \Upsilon \geq P_j^{\max}, \end{cases} \end{aligned} \quad (63)$$

where $\Upsilon = \frac{|\mathbf{h}_{rb}^H \Theta_r \mathbf{H}_{AR} \mathbf{w}_b|^2 - (2^{R_b} - 1)(|\mathbf{h}_{rb}^H \Theta_r \mathbf{H}_{AR} \mathbf{w}_c|^2 + \sigma_b^2)}{(2^{R_b} - 1)|\mathbf{h}_{rb}^H \Theta_r \mathbf{h}_{rc}^*|^2}$.

Similarly, when the required transmission rate between Alice and Carol is chosen as R_c , the communication outage probability at Carol under the randomness of the jamming power P_j and the self-interference channel h_{cc} is derived as

$$\begin{aligned} \delta_{AC} &= \Pr(C_c < R_c) \\ &= \Pr\left(|g_{cc}|^2 P_j > \frac{\Gamma}{\phi}\right) \\ &= \begin{cases} \int_0^{P_j^{\max}} \int_{\frac{\Gamma}{\phi y}}^{+\infty} e^{-x} \frac{1}{P_j^{\max}} dx dy, & \Gamma \geq 0, \\ 1, & \Gamma < 0, \end{cases} \\ &= \begin{cases} e^{-\frac{\Gamma}{\phi P_j^{\max}}} + \frac{\Gamma}{\phi P_j^{\max}} \text{Ei}\left(-\frac{\Gamma}{\phi P_j^{\max}}\right), & \Gamma \geq 0, \\ 1, & \Gamma < 0, \end{cases} \end{aligned} \quad (64)$$

where $\Gamma = \frac{|\mathbf{h}_{rc}^H \Theta_t \mathbf{H}_{AR} \mathbf{w}_c|^2 - (2^{R_c} - 1)(|\mathbf{h}_{rc}^H \Theta_t \mathbf{H}_{AR} \mathbf{w}_b|^2 + \sigma_c^2)}{(2^{R_c} - 1)}$.

REFERENCES

- [1] A. Chorti, A. N. Barreto, S. Köpsell, M. Zoli, M. Chaffi, P. Sehier, G. Fettweis, and H. V. Poor, "Context-aware security for 6G wireless: The role of physical layer security," *IEEE Commun. Standards Mag.*, vol. 6, no. 1, pp. 102–108, 2022.
- [2] M. Cui, G. Zhang, and R. Zhang, "Secure wireless communication via intelligent reflecting surface," *IEEE Wireless Commun. Lett.*, vol. 8, no. 5, pp. 1410–1414, 2019.
- [3] X. Hu, P. Mu, B. Wang, and Z. Li, "On the secrecy rate maximization with uncoordinated cooperative jamming by single-antenna helpers," *IEEE Trans. Veh. Technol.*, vol. 66, no. 5, pp. 4457–4462, 2017.
- [4] T.-X. Zheng, Z. Yang, C. Wang, Z. Li, J. Yuan, and X. Guan, "Wireless covert communications aided by distributed cooperative jamming over slow fading channels," *IEEE Trans. Wireless Commun.*, vol. 20, no. 11, pp. 7026–7039, 2021.
- [5] X. Chen, W. Sun, C. Xing, N. Zhao, Y. Chen, F. R. Yu, and A. Nallanathan, "Multi-antenna covert communication via full-duplex jamming against a warden with uncertain locations," *IEEE Trans. Wireless Commun.*, vol. 20, no. 8, pp. 5467–5480, 2021.
- [6] S. Yan, X. Zhou, J. Hu, and S. V. Hanly, "Low probability of detection communication: Opportunities and challenges," *IEEE Wireless Commun.*, vol. 26, no. 5, pp. 19–25, 2019.
- [7] B. A. Bash, D. Goeckel, and D. Towsley, "Limits of reliable communication with low probability of detection on AWGN channels," *IEEE J. Sel. Areas Commun.*, vol. 31, no. 9, pp. 1921–1930, 2013.
- [8] D. Goeckel, B. Bash, S. Guha, and D. Towsley, "Covert communications when the warden does not know the background noise power," *IEEE Commun. Lett.*, vol. 20, no. 2, pp. 236–239, 2015.
- [9] J. Wang, W. Tang, Q. Zhu, X. Li, H. Rao, and S. Li, "Covert communication with the help of relay and channel uncertainty," *IEEE Wireless Commun. Lett.*, vol. 8, no. 1, pp. 317–320, 2018.
- [10] J. Hu, S. Yan, X. Zhou, F. Shu, and J. Li, "Covert wireless communications with channel inversion power control in rayleigh fading," *IEEE Trans. Veh. Technol.*, vol. 68, no. 12, pp. 12 135–12 149, 2019.
- [11] L. Tao, W. Yang, S. Yan, D. Wu, X. Guan, and D. Chen, "Covert communication in downlink NOMA systems with random transmit power," *IEEE Wireless Commun. Lett.*, vol. 9, no. 11, pp. 2000–2004, 2020.
- [12] K. Li, P. A. Kelly, and D. Goeckel, "Optimal power adaptation in covert communication with an uninformed jammer," *IEEE Trans. Wireless Commun.*, vol. 19, no. 5, pp. 3463–3473, 2020.
- [13] K. Shahzad, X. Zhou, and S. Yan, "Covert communication in fading channels under channel uncertainty," in *Proc. IEEE Veh. Technol. Conf (VTC Spring)*, 2017, pp. 1–5.
- [14] R. Ma, W. Yang, L. Tao, X. Lu, Z. Xiang, and J. Liu, "Covert communications with randomly distributed wardens in the finite blocklength regime," *IEEE Trans. Veh. Technol.*, vol. 71, no. 1, pp. 533–544, 2021.
- [15] T.-X. Zheng, H.-M. Wang, D. W. K. Ng, and J. Yuan, "Multi-antenna covert communications in random wireless networks," *IEEE Trans. Wireless Commun.*, vol. 18, no. 3, pp. 1974–1987, 2019.
- [16] K. Shahzad, X. Zhou and S. Yan, "Covert wireless communication in presence of a multi-antenna adversary and delay constraints," *IEEE Trans. Veh. Technol.*, vol. 68, no. 12, pp. 12 432–12 436, 2019.
- [17] Q. Wu and R. Zhang, "Towards smart and reconfigurable environment: Intelligent reflecting surface aided wireless network," *IEEE Commun. Mag.*, vol. 58, no. 1, pp. 106–112, 2019.
- [18] X. Hu, C. Masouros, and K.-K. Wong, "Reconfigurable intelligent surface aided mobile edge computing: From optimization-based to location-only learning-based solutions," *IEEE Trans. Commun.*, vol. 69, no. 6, pp. 3709–3725, 2021.
- [19] X. Lu, E. Hossain, T. Shafique, S. Feng, H. Jiang, and D. Niyato, "Intelligent reflecting surface enabled covert communications in wireless networks," *IEEE Netw.*, vol. 34, no. 5, pp. 148–155, 2020.
- [20] X. Zhou, S. Yan, Q. Wu, F. Shu, and D. W. K. Ng, "Intelligent reflecting surface (IRS)-aided covert wireless communications with delay constraint," *IEEE Trans. Wireless Commun.*, vol. 21, no. 1, pp. 532–547, 2021.
- [21] X. Chen, T.-X. Zheng, L. Dong, M. Lin, and J. Yuan, "Enhancing MIMO covert communications via intelligent reflecting surface," *IEEE Wireless Commun. Lett.*, vol. 11, no. 1, pp. 33–37, 2021.
- [22] C. Wang, Z. Li, J. Shi, and D. W. K. Ng, "Intelligent reflecting surface-assisted multi-antenna covert communications: Joint active and passive beamforming optimization," *IEEE Trans. Commun.*, vol. 69, no. 6, pp. 3984–4000, 2021.

- [23] Y. Liu, X. Mu, J. Xu, R. Schober, Y. Hao, H. V. Poor, and L. Hanzo, "STAR: Simultaneous transmission and reflection for 360° coverage by intelligent surfaces," *IEEE Wireless Commun.*, vol. 28, no. 6, pp. 102–109, 2021.
- [24] X. Mu, Y. Liu, L. Guo, J. Lin, and R. Schober, "Simultaneously transmitting and reflecting (STAR) RIS aided wireless communications," *IEEE Trans. Wireless Commun.*, vol. 21, no. 5, pp. 3083–3098, 2022.
- [25] Y. Han, N. Li, Y. Liu, T. Zhang, and X. Tao, "Artificial noise aided secure NOMA communications in STAR-RIS networks," *IEEE Wireless Commun. Lett.*, 2022.
- [26] Z. Zhang, J. Chen, Y. Liu, Q. Wu, B. He, and L. Yang, "On the secrecy design of STAR-RIS assisted uplink NOMA networks," *IEEE Trans. Wireless Commun.*, vol. 21, no. 12, pp. 11 207–11 221, 2022.
- [27] C. Wu, C. You, Y. Liu, X. Gu, and Y. Cai, "Channel estimation for STAR-RIS-aided wireless communication," *IEEE Commun. Lett.*, vol. 26, no. 3, pp. 652–656, 2021.
- [28] D. Kim, H. Lee, and D. Hong, "A survey of in-band full-duplex transmission: From the perspective of PHY and MAC layers," *IEEE Commun. Surveys Tuts.*, vol. 17, no. 4, pp. 2017–2046, 2015.
- [29] X. Zhou, S. Yan, J. Hu, J. Sun, J. Li, and F. Shu, "Joint optimization of a UAV's trajectory and transmit power for covert communications," *IEEE Trans. Signal Process.*, vol. 67, no. 16, pp. 4276–4290, 2019.
- [30] J. Evans and D. N. C. Tse, "Large system performance of linear multiuser receivers in multipath fading channels," *IEEE Trans. Inf. Theory.*, vol. 46, no. 6, pp. 2059–2078, 2000.
- [31] Y. Wu, R. Schober, D. W. K. Ng, C. Xiao, and G. Caire, "Secure massive MIMO transmission with an active eavesdropper," *IEEE Trans. Inf. Theory.*, vol. 62, no. 7, pp. 3880–3900, 2016.
- [32] Q. Wu and R. Zhang, "Towards smart and reconfigurable environment: Intelligent reflecting surface aided wireless network," *IEEE Commun. Mag.*, vol. 58, no. 1, pp. 106–112, 2020.
- [33] Z. Ding, R. Schober, and H. V. Poor, "On the impact of phase shifting designs on IRS-NOMA," *IEEE Wireless Commun. Lett.*, vol. 9, no. 10, pp. 1596–1600, 2020.
- [34] Z.-Q. Luo, W.-K. Ma, A. M.-C. So, Y. Ye, and S. Zhang, "Semidefinite relaxation of quadratic optimization problems," *IEEE Signal Process. Mag.*, vol. 27, no. 3, pp. 20–34, 2010.
- [35] M. Grant and S. Boyd, "CVX: Matlab software for disciplined convex programming, version 2.1," 2014.
- [36] Q. Wu and R. Zhang, "Intelligent reflecting surface enhanced wireless network via joint active and passive beamforming," *IEEE Trans. Wireless Commun.*, vol. 18, no. 11, pp. 5394–5409, 2019.
- [37] Q. Wu and R. Zhang, "Intelligent reflecting surface enhanced wireless network: Joint active and passive beamforming design," in *Proc. IEEE Global Commun. Conf. (GLOBECOM)*. IEEE, 2018, pp. 1–6.
- [38] A. Zappone, E. Jorswieck *et al.*, "Energy efficiency in wireless networks via fractional programming theory," *Found. Trends Commun. Inf. Theory.*, vol. 11, no. 3–4, pp. 185–396, 2015.
- [39] J. Nocedal and S. J. Wright, *Numerical optimization*. New York, NY, USA: Springer, 2006.
- [40] X. Hu, L. Wang, K. Wong, M. Tao, Y. Zhang, and Z. Zheng, "Edge and central cloud computing: A perfect pairing for high energy efficiency and low-latency," *IEEE Trans. Wireless Commun.*, vol. 19, no. 2, pp. 1070–1083, 2020.
- [41] S. Boyd, S. P. Boyd, and L. Vandenberghe, *Convex optimization*. Cambridge, U.K.:Cambridge Univ. Press, 2004.
- [42] D. Bharadia, E. McMillin, and S. Katti, "Full duplex radios," in *Proc. ACM SIGCOMM*, 2013, pp. 375–386.
- [43] K. Svanberg, "MMA and GCMMA-two methods for nonlinear optimization," *Tech. Rep. Optim. Theory.*, vol. 1, 2007.
- [44] K. Svanberg, "A class of globally convergent optimization methods based on conservative convex separable approximations," *SIAM J. Optim.*, vol. 12, no. 2, pp. 555–573, 2002.